E AND F-REGION CHEMISTRY AND HIGH-LATITUDE IONOSPHERE

Daniel A. Hamlin, et al

Science Applications, Incorporated

Prepared for:

Office of Naval Research

28 February 1974

UNCLASSIFIED

SECURITY CLASSIFICATION OF THIS PAGE (When Data Entered)

AD 776 236

REPORT DOCUMENTATION PAGE		READ INSTRUCTIONS BEFORE COMPLETING FORM
1. REPORT NUMBER	2. GOVT ACCESSION NO.	3. RECIPIENT'S CATALOG NUMBER
4. TITLE (and Subtitle) E- and F-Region Chemistry and High-Latitude Ionosphere		5. TYPE OF REPORT & PERIOD COVERED Final Technical Report 15 Jan 72 - 31 Dec 73 6. PERFORMING ORG. REPORT NUMBER SAI-74-537-LJ
7. AUTHOR(s) Daniel A. Hamlin, Benjamin F. Myers, Melvin R. Schoonover and John I. Valerio		8. CONTRACT OR GRANT NUMBER(s) N00014-72-C-0292-[redacted] ARPA Order No. 2020
9. PERFORMING ORGANIZATION NAME AND ADDRESS Science Applications, Inc. 1200 Prospect Street La Jolla, California 92037		10. PROGRAM ELEMENT, PROJECT, TASK AREA & WORK UNIT NUMBERS Program Code 2F10
11. CONTROLLING OFFICE NAME AND ADDRESS Defense Advanced Research Projects Agency 1400 Wilson Boulevard Arlington, Virginia 22209		12. REPORT DATE 28 February 1974 13. NUMBER OF PAGES 105
14. MONITORING AGENCY NAME & ADDRESS(if different from Controlling Office) Office of Naval Research 800 North Quincy Street Arlington, Virginia 22217		15. SECURITY CLASS. (of this report) UNCLASSIFIED 15a. DECLASSIFICATION/DOWNGRADING SCHEDULE

16. DISTRIBUTION STATEMENT (of this Report)

17. DISTRIBUTION STATEMENT (of the abstract entered in Block 20, if different from Report)

18. SUPPLEMENTARY NOTES
Section 2 has been submitted for publication
Section 3 will be submitted for publication
Section 4 has been submitted for publication
Section 5 has been published

19. KEY WORDS (Continue on reverse side if necessary and identify by block number)

Ionosphere
E- and F-region
Photoelectron flux spectra
Photoelectron slowing down
Error propagation in chemical systems
Electron heating
Dissociative-recombination temperature dependence

20. ABSTRACT (Continue on reverse side if necessary and identify by block number)
Four separate detailed studies of the chemistry and related microscopic processes of the ionosphere have been made. It is shown that: (a) electron-flux spectra, calculated with a discrete energy-loss model for dawn conditions at altitudes of 180, 200, and 250 km, agree well with recent observations by Hays and Sharp (1973), but a discrepancy occurs between the calculated rate of electron formation by photoionization and collisional ionization and the loss rate deduced from the measured electron and ion densities. (b) Based on statistical error propagation in an E-region

DD FORM 1 JAN 73 1473 EDITION OF 1 NOV 65 IS OBSOLETE

UNCLASSIFIED

SECURITY CLASSIFICATION OF THIS PAGE (When Data Entered)

Block 20 continued

chemical-kinetics system, the fractional standard derivations (FSD) of density distributions are, in general, less than twice the common value of the FSD, f_{sk}, assigned to the rate-coefficient error distributions, provided $f_{sk} \leq 0.45$; the mean densities are relatively insensitive to the rate-coefficient uncertainties. (c) The loss of ionospheric electrons by dissociative recombination effectively heats the electron gas at a rate which is a few per cent of the main heating rate due to photoelectrons but which exceeds some of the rates for minor cooling processes frequently included in energy-balance studies. (d) The temperature dependence for the dissociative recombination of NO^+ customarily used in E- and F-region models is not correct.

SAI-74-537-LJ

FINAL TECHNICAL REPORT*

E- AND F-REGION CHEMISTRY AND HIGH-LATITUDE IONOSPHERE

Prepared
under
Contract N00014-72-C-0292-[redacted]
ARPA Order No. 2020, Program Code 2F10

by
D. A. Hamlin, Principal Investigator, Tel. (714) 459-0211
B. F. Myers, M. R. Schoonover, and J. I. Valerio

The views and conclusions contained in this document are those of the authors and should not be interpreted as necessarily representing the official policies, either expressed or implied, of the Advanced Research Projects Agency or the U. S. Government.

Effective Period of Contract:
15 January 1972 to 31 December 1973
Amount of Contract: $138,883

Scientific Officer:
Dr. John G. Dardis
Physics Programs
Phys. Sci. Div., ONR

Sponsored by
Advanced Research Projects Agency
ARPA Order No. 2020 dated 27 December 1971

SCIENCE APPLICATIONS, LA JOLLA, CALIFORNIA
ALBUQUERQUE • ANN ARBOR • ARLINGTON • ATLANTA • BOSTON • CHICAGO • HUNTSVILLE
LOS ANGELES • McLEAN • PALO ALTO • SANTA BARBARA • SUNNYVALE • TUCSON
P.O. Box 2351, 1200 Prospect Street, La Jolla, California 92037

*Form Approved Budget Bureau No. 22-R0293

TABLE OF CONTENTS

SECTION 1

INTRODUCTION

Introduction

Early in 1972, the Advanced Research Projects Agency initiated a several-year program to develop a comprehensive global model of the ionosphere. As one facet of the overall program, Science Applications, Inc. (SAI) emphasized detailed studies of the chemistry and related microscopic processes for the quiet, mid-latitude E- and F-regions of the ionosphere, and took an important step toward considering high-latitude ionospheric problems.

SAI first modified its computer code (called CHIEF) for chemistry of ionization in the E- and F-regions. CHIEF is quite elaborate, carrying about 25 species (including excited states) and several hundred reactions. This code was originally developed for studying an artificially-perturbed atmosphere. The modification consisted mainly in providing the code with a solar source of UV, EUV, and x rays during the day and a nighttime ionization source. As a step toward making theoretical predictions with a computer program about the chemical, optical, and other microscopic processes in a natural electron aurora, SAI developed an electron slowing-down routine — with account of discrete-energy losses instead of the more usual and approximate continuous slowing-down treatment — and incorporated the routine into the large ionospheric chemistry code, now called SOLAKEM. This code was tested by applying it to the experimental conditions appropriate for the recently-reported rocket flight of Hays and Sharp [J. Geophys. Res. 78, 1153 (1973)] who have made the most accurate measurements to date of the solar-produced photoelectron-flux spectra in the altitude range from 180 to 250 km. SAI's computed photoelectron-flux spectra are in very good agreement with the Hays-Sharp data. The details of this calculation are given in Section 2.

Additional, less extensive studies, also to be published, included (a) determining, for a 12-species, 25-reaction, E- and F-region chemical kinetics code, the uncertainties in species densities due to uncertainties in the rate coefficients for the reactant species (Section 3), (b) recognizing that dissociative recombination of molecular ions and electrons influence the ionospheric electron temperature to a larger extent than some of the effects usually included in computing the electron temperature (Section 4), and (c) noting that the temperature dependence for the dissociative recombination of NO^+ customarily used in E- and F-region ionospheric models is incorrect (Section 5).

SECTION 2

CALCULATED AND OBSERVED PHOTOELECTRON-FLUX SPECTRA AT DAWN

Calculated and Observed Photoelectron-Flux Spectra at Dawn

B. F. Myers, D. A. Hamlin, and M. R. Schoonover
Science Applications, Inc., La Jolla, California 92037, U. S. A.

Abstract — Electron-flux spectra have been calculated for dawn conditions at altitudes of 180, 200, and 250 km and compared with recent observations by Hays and Sharp (1973) on a payload launched from White Sands, New Mexico, U.S.A. on February 8, 1971. A discrete energy-loss model was used in the calculations and good agreement is found between the calculated and measured spectra. The prominent structural features in the observed spectra are reproduced in the calculated spectra and are analyzed. A discrepancy is found between the calculated rate of electron formation by photoionization and collisional ionization and the loss rate deduced from the measured electron and ion densities. No definitive explanation of this discrepancy has been found, either in terms of omitted absorption or transport processes or in terms of uncertainties in data employed in the calculations.

1. INTRODUCTION

Measurements of photoelectron-flux spectra have recently been made (Hays and Sharp, 1973) by using instrumentation which permits meaningful measurements in the range of electron energies from below one electron volt (eV) to several tens of electron volts. These flux spectra have good

resolution and display interesting structural features, which prompted us to test a method of calculating the electron-flux spectra. An additional feature of the experiment was the simultaneous measurements of the charged particle densities; these provide further tests for the calculations.

The electron-flux spectra were calculated by a discrete energy-loss procedure with an energy resolution compatible with the observations. The procedure is part of a larger computer code which is used to describe the chemical and energetic transformations in the E and F regions of the ionosphere over short time intervals. We report here on a comparison of the calculated and observed electron-flux spectra and on difficulties in computing energy and density profiles during the observations.

2. METHOD OF CALCULATION

A simple method was used to treat the discrete energy-loss processes undergone by photoelectrons formed by solar radiation incident on atmospheric species. The method is based on the assumptions that a steady state for electrons, sorted into a set of energy groups, is quickly established after photoabsorption and that electrons only lose energy in each interaction process until a specified energy limit is reached. In the present application, the further simplifications of local energy deposition and isotropic electron fluxes are invoked. The total set of electrons is divided into a "high-energy" slowing-down subset

comprising electrons with 30 discrete energies between 1 and 10^3 eV and a "thermal" subset characterized by an electron temperature. The relation between the subsets is shown in Section 2.2 to be in accord with a recent self-consistent treatment (Krinberg, 1973).

2.1 High-energy electrons

Application of the steady-state assumption to the subset of high-energy electrons leads to the following expression for the density of electrons in energy group j,

$$[e_j\ (cm^{-3}\ bin^{-1})] = P_j/L_j \quad , \tag{1}$$

where the production rate is

$$P_j(cm^{-3}\ sec^{-1}\ bin^{-1}) = \underbrace{\sum_S \sum_i \varphi(i,t)\ \sigma(i,S)\ b_p(i,j,S)\ [S]}_{\text{photoabsorption}}$$

$$+ \underbrace{\sum_S \sum_{k>j} [e_k]\ v_k\ \sigma_{xd}(k,S)\ b_{xd}(k,j,S)\ [S]}_{\text{excitation, dissociation, and dissoc. excit.}}$$

$$+ \underbrace{\sum_S \sum_{k>j} [e_k]\ v_k\ \sigma_i(k,S)\ b_i(k,j,S)\ [S]}_{\text{ionization and dissoc. ioniz.}}$$

$$+ \underbrace{C_{j+1,j}\ [e_{j+1}]}_{\text{loss to thermal electrons}} \tag{2}$$

and the loss-rate coefficient is

$$L_j(\text{sec}^{-1}) = v_j \sum_S \left\{ [1 - b_{xd}(j,j,S)]\, \sigma_{xd}(j,S) + [1 - b_i(j,j,S)]\, \sigma_i(j,S) \right\} [S] + C_{j,j-1} \quad . \qquad (3)$$

The terms on the right hand side of equation (2) refer, respectively, to the processes of photoabsorption, excitation and dissociation (including dissociative excitation), ionization (including dissociative ionization), and loss of energy to thermal electrons by the high-energy electrons; the latter three processes are also represented by terms in L_j, given by equation (3). The photoabsorption term gives the rate of forming electrons in energy group j by absorption of group-i photons; $\varphi(i,t)$ is the group-i photon flux at time t, $\sigma(i,S)$ is the photoionization cross-section for species S absorbing group-i photons, and $b_p(i,j,S)$ is the probability that a group-j electron is formed when species S absorbs a group-i photon. The excitation and dissociation term gives the rate of forming electrons in group j by group-k electrons impacting on S; v_k is the velocity of a group-k electron, $\sigma_{xd}(k,S)$ is the cross section for excitation, dissociation, or dissociative excitation of S by group-k electrons, and $b_{xd}(k,j,S)$ is the probability of forming a group-j electron when a group-k electron interacts with S. The ionization term gives the rate of forming group-j electrons by group-k electrons interacting with S; $\sigma_i(k,S)$ is the cross section for group-k electrons ionizing S, and $b_i(k,j,S)$ is the probability

of forming group-j electrons by group-k electrons interacting with S. The quantity $C_{j+1,j}$ is the rate at which electrons leave group j+1 and enter group j as a result of energy loss to thermal electrons. Further consideration of $C_{j+1,j}$ as well as of the probability factors $b_{xd}(j,j,S)$ and $b_i(j,j,S)$ of equation (3) will be given below.

Ten energy groups per decade of electron energy were established, as shown in Table 1. The energy groups span approximately equal intervals on a logarithmic scale; ΔU_j is the width of group j and U_j is the characteristic energy.

The resolution of the energy-group scale, $\Delta U_j/U_j$, is slightly above 20 per cent whereas the resolution of the photoelectron spectrometer used in the observations (Hays and Sharp, 1973) being modeled was 10 per cent. The energy resolution in the model could be increased by increasing the number of groups, but comparison of calculated and observed electron fluxes, as shown in Section 4.1, indicates no need for such change in the present application.

A problem arises from two requirements imposed on the model. First, the model must accurately describe the discrete energy losses in relevant physical processes and second, the model must employ an arbitrary set of energy groups and related characteristic energies. These requirements, by themselves, are not compatible, in general, since the discrete energy loss by an electron in a particular physical process is unlikely to have a value equal to a difference in characteristic energies.

This problem is overcome by "splitting" electrons, i.e., deriving probabilities that the outgoing electron in the physical process will assume characteristic energies which lie on either side of the true value of the electron energy. The probabilities are derived on the basis of conservation of energy and of the total (free plus bound) number of electrons.

For photoionization, the energy of the outgoing electron, $E_e(i)$, is

$$E_e(i) = E_p(i) - E(S') \quad , \tag{4}$$

where $E_p(i)$ is the energy of the group-i photon and $E(S')$ is the energy of the product ion, S'. If

$$U_j < E_e(i) < U_{j+1} \quad , \qquad j \geq 1 \tag{5}$$

then the probabilities for the electrons are

$$b_p(i,j,S) = \left[\frac{U_{j+1} - E_p(i)}{U_{j+1} - U_j}\right] b(i,S,S') \tag{6}$$

and

$$b_p(i,j+1,S) = b(i,S,S') - b_p(i,j,S) \quad , \tag{7}$$

where $b(i,S,S')$ is the probability that product S' is formed by target S absorbing a group-i photon. This probability is specified by experimental data and is further considered in Section 3.1. If, instead of the inequality of equation (5),

$$E_e(i) < U_1 = 1.1 \text{ eV} \quad , \tag{8}$$

the electron is added to the thermal subset with probability

$$b_p(i, 0, S) = b(i, S, S') \tag{9}$$

and energy $E_e(i) \cdot b(i, S, S')$ is added to the energy of the thermal subset.

For an excitation, dissociation, or dissociative excitation event, the procedure for deriving probabilities, $b_{xd}(k, j, S)$, is identical to the procedure described for photoionization events. The energy of the outgoing electron, $E_e(xd)$, is

$$E_e(xd) = U_k - E(S') \tag{10}$$

where U_k is the energy of the impacting electron and $E(S')$ is the energy of the product S'. Equations (5) through (9) apply in this case when the quantities $E_p(i)$, $b_p(i, j, S)$, $b_p(i, j+1, S)$, and $b(i, S, S')$ are replaced by $E_e(xd)$, $b_{xd}(k, j, S)$, $b_{xd}(k, j+1, S)$, and $b_{xd}(k, S, S')$, respectively. The quantity $b_{xd}(k, S, S')$ is the probability for forming product S' by a group-k electron interacting with target S; like $b(i, S, S')$, $b_{xd}(k, S, S')$ also is available from experimental data. In calculations of $b_p(i, j, S)$ and $b_{xd}(k, j, S)$, the numerical accuracy was of an order to produce errors in energy conservation of 10^{-5} eV or less, for each event.

For the ionization term in equation (2), a single ionization event is considered in which there are two outgoing electrons; the lower-energy electron is named the "secondary" and the other, the "degraded primary" electron. Both electrons are described by differential energy spectra (Opal et al., 1971). These experimental spectra are only approximated by the procedure employed here in obtaining values of

$b_i(k, j, S)$. For the discrete set of characteristic energies, U_j, and energy-group wi.' ΔU_j, the differential probability, i.e., probability per eV, for forming a secondary electron with specified energy is chosen to satisfy the relation

$$\sum_{j=0}^{j_{max}} P_s(j) \cdot \Delta U_j = P_s(j_{max}) \sum_{j=0}^{j_{max}} \Delta U_j \equiv P_s(j_{max})\, W(j_{max}) = 1 \ , \quad (11)$$

where the differential probability for the secondary electron, $P_s(j_{max})$ is assumed to be constant over the range of energies assigned to the secondary electrons. $P_s(j_{max})$ is restricted to certain values which can be deduced from equation (11) by using Table 1 for values of W_j. We let j_{max} be determined indirectly by choosing the largest possible value of $P_s(j_{max})$ that is less than the differential probability, P, for the secondary-electron energy, E_s, given by

$$P(E_s) \approx \left\{ \overline{E} \arctan\left[\frac{U_k - I - X}{2\overline{E}}\right]\left[1 + \left(\frac{E_s}{\overline{E}}\right)^2\right]\right\}^{-1} \ , \quad (12)$$

when evaluated for $E_s = 0$. The functional form in equation (12) is that previously used by Opal et al. (1971) to describe secondary-electron spectra; here, we slightly generalized by replacing the ionization potential I by I+X where X is the electronic excitation energy of the product ion. The quantity $\overline{E}$ is a shape parameter which is assumed to be constant for a given target, as it varies only slowly as a function of U_k; values of $\overline{E}$ are discussed in Section 3.3.

The differential probabilities defining the spectrum of degraded primary electrons, P'_d and P''_d, are calculated on the basis of energy conservation and unit, total probability; two differential probabilities for the degraded primaries are used to ensure that the conservation conditions can be satisfied within a tolerably small error, in spite of the fixed values of ΔU_j. Thus,

$$(U_k - I - X) - P_s(j_{max})\left[\sum_{j=0}^{j_{max}} \Delta U_j \cdot U_j\right]_s = P'_d\left[\sum_k \Delta U_k \cdot U_k\right]_{d'} + P''_d\left[\sum_\ell \Delta U_\ell \cdot U_\ell\right]_{d''} \tag{13}$$

and

$$P'_d \cdot \left[\sum_k \Delta U_k\right]_{d'} + P''_d \cdot \left[\sum_\ell \Delta U_\ell\right]_{d''} = 1 \ . \tag{14}$$

The ranges of the indices k and ℓ are selected to provide positive values of P'_d and P''_d and, hopefully, $P''_d > P'_d$; the inequality is in accord with observations of an increasing differential probability with increasing energy for the degraded primary electron (Opal et al., 1971). The ranges of the indices k and ℓ are selected by an algorithm which also may adjust j_{max} to satisfy the conditions on the differential probabilities and additionally select the maximum value of $P''_d - P'_d$. In some cases, the inequality $P''_d > P'_d$ cannot be satisfied and in these cases the smallest value of $P'_d - P''_d$ is chosen from the sets of P'_d, P''_d which are solution sets of equations (13) and (14).

Two examples of the use of the method for computing the differential probability spectra in a single ionization event are shown in Fig. 1; in the case for which the primary energy is 45 eV, the inequality $P''_d > P'_d$ could not be satisfied.

The relation between $b_i(k, j, S)$ of equation (2) and the differential probabilities $P_s(j_{max})$, P'_d, and P''_d is

$$b_i(k, j, S) = P_j \, \Delta U_j \, b(k, S, S') \tag{15}$$

where P_j, denoting $P_s(j_{max})$, P'_d, or P''_d, is the differential probability for the group with characteristic energy U_j, ΔU_j is the width of the group, and $b(k, S, S')$ is the probability for forming an ion S' when a group-k electron interacts with target S; the probability $b(k, S, S')$ is available from experimental data and is considered in Section 3.3.

The probability factors in equation (3), $b_{xd}(j, j, S)$ and $b_i(j, j, S)$, in which the incident and an outgoing electron are assigned to the same energy group, take account of those events in which the electron energy loss is smaller than the difference $U_j - U_{j-1}$. These factors appear in equation (3) as a result of factoring the density $[e_j]$.

The loss-rate coefficient for energy loss to the thermal subset of electrons appearing in equations (2) and (3) is calculated with the approximate expression (Schunk and Hays, 1971)

$$C_{j,j-1} = \frac{7.73 \times 10^{-6}\,[e_o]}{\delta U_j\,\langle\sqrt{U_j}\rangle} \begin{cases} \ln\left[\dfrac{2.531 \times 10^{10}\,U_j^{\frac{3}{2}}}{[e_o]^{\frac{1}{2}}}\right], & U_j < 13.62 \text{ eV} \\ \ln\left[\dfrac{5.387 \times 10^{10}\,U_j}{[e_o]^{\frac{1}{2}}}\right], & U_j > 13.62 \text{ eV} \end{cases} \tag{16a}$$

where

$$\delta U_j = \begin{cases} U_j - U_{j-1}, & j \geq 2 \\ U_1 - 1, & j = 1, \end{cases} \tag{16b}$$

$$\langle\sqrt{U_j}\rangle = \begin{cases} 0.5\,(\sqrt{U_j} + \sqrt{U_{j-1}}), & j \geq 2 \\ 0.5\,(\sqrt{U_1} + 1), & j = 1, \end{cases} \tag{16c}$$

and $[e_o] \equiv [e_{th}]$ is the density of electrons in the thermal subset. The form of equation (16) is valid for electron temperatures below 2500 °K. For the conditions of the present calculations, the energy loss per collision with the thermal subset of electrons is less than the energy difference between groups; this is the basis for the arguments (j, j-1) of the energy-loss coefficient of equation (16).

2.2 Thermal electrons

The thermal subset of electrons has contributions from energy-degraded, high-energy electrons as a result of the loss processes included in equation (2), as well as from photoabsorption events. The rate of

increase in the thermal electron density is given by equation (2) with j understood to represent the thermal subset.

The total electron density in each of the lower-energy groups of Table 1, $[e_{t,j}]$, includes a significant contribution from the thermal subset of electrons for the conditions of the observations being modeled. The fraction of the thermal electrons in group j is

$$\frac{[e_{th,j}]}{[e_{th}]} = \alpha(y_j) - \alpha(y_{j-1}) \quad , \tag{17}$$

where $[e_{th,j}]$ is the density of thermal electrons in group j,

$$\alpha(x) = \mathrm{erf}(\sqrt{x}) - \frac{2}{\sqrt{\pi}} \sqrt{x}\ e^{-x} \quad , \tag{18}$$

erf(z) is the error function, and

$$y_j = W_j/\theta \quad , \tag{19}$$

where W_j is the upper-edge energy of group j and θ is the electron temperature. Equation (18) is based on a Maxwellian distribution of energy,

$$f(E) = \frac{2}{\sqrt{\pi}} \frac{\sqrt{E}}{\theta^{\frac{3}{2}}} e^{-E/\theta} \quad . \tag{20}$$

The total electron density in group j is then

$$[e_{t,j}] = [e_j] + [e_{th,j}] \quad . \tag{21}$$

The two foregoing paragraphs describe our method for treating the interaction of the high-energy electrons with the ambient electrons, which is in good agreement with a rigorous, self-consistent treatment (Krinberg,

1973) of this interaction. To illustrate this agreement we have applied our method to a sample problem considered by Krinberg (1973) in which the photoelectrons lose their energy locally by only Coulomb collisions with ambient electrons; the photoelectron production spectrum is $q = q_o \exp(-E/E_o)$, with $q_o = 10^2$ cm^{-3} sec^{-1} and $E_o = 10$ eV, and the electron temperature and density are $\theta = 0.25$ eV and $[e_{th}] = 5 \times 10^5$ cm^{-3}, respectively. For this sample problem the production rate is

$$P_j(\text{cm}^{-3}\ \text{sec}^{-1}\ \text{bin}^{-1}) = q_o(e^{-w_{j-1}} - e^{-w_j}) + C_{j+1,j}\,[e_{j+1}] \ , \qquad (22a)$$

where

$$w_j = W_j/E_o \ , \qquad (22b)$$

and the loss-rate coefficient is

$$L_j(\text{sec}^{-1}) = C_{j,j-1} \ . \qquad (23)$$

For the slowing-down electrons, the isotropic, steradianal, differential-energy electron flux is

$$\psi_j(\text{cm}^{-2}\ \text{sec}^{-1}\ \text{eV}^{-1}\ \text{sr}^{-1}) = \frac{v_j\,[e_j]}{4\pi\,\Delta U_j} \ , \qquad (24)$$

where v_j is the electron velocity corresponding to U_j. The corresponding flux for a Maxwellian distribution is

$$\psi_M(E) = \frac{v\,f(E)\,[e_{th}]}{4\pi} \ , \qquad (25)$$

and the total flux is

$$\psi_{t,j} = \psi_j + \psi_M(U_j) \quad . \tag{26}$$

In Fig. 2 the triangular points, representing the total flux, were computed from equation (26); the circular points, representing only the slowing-down flux, were computed from equation (24). The curves in Fig. 2 are based on Krinberg's (1973) equation (11), modified for consistency with his text; the solid curve represents the total flux and the dashed curve, based on only the second term of Krinberg's (1973) equation (11), neglects the contribution of the thermal electrons and includes only the slowing-down flux. The agreement between the two methods for the total flux is seen to be quite adequate.

The types of processes undergone by the thermal subset of electrons are the same as for the high-energy subset, except for energy limitations; specific processes are discussed in Section 3.

2.3 Species and energy densities

As a result of the processes involving the photoelectrons, species are transformed and energy is redistributed. Here, these changes are distinguished from the additional changes in species and energy densities involving the ambient electrons, chemical reactions, and transport of species and energy. This distinction permits some understanding of the effect of the formation of photoelectrons, except for those created directly into the thermal subset, for the conditions of the observations (Hays and Sharp, 1973). The rate of increase in the total electron density,

$$[e] = [e_{th}] + \sum_{j \geq 1} [e_j] \quad , \tag{27}$$

due to photoelectrons, is

$$\frac{d[e]}{dt} = \underbrace{\sum_S \sum_i \varphi(i,t)\, \sigma(i,S)\, [S]}_{\text{photoabsorption}}$$

$$+ \underbrace{\sum_S \sum_{j \geq 1} [e_j]\, v_j\, \sigma_i(j,S)\, [S]}_{\text{ionization}} \quad . \tag{28}$$

The rates for loss of species S and gain of species S′, due to photoelectrons, are

$$-\frac{d[S]}{dt} = \sum_i \varphi(i,t)\, \sigma(i,S)\, [S] + \sum_{j \geq 1} [e_j]\, v_j [\sigma_{xd}(j,S) + \sigma_i(j,S)]\, [S] \tag{29}$$

$$\frac{d[S']}{dt} = \sum_S \sum_i \varphi(i,t)\, \sigma(i,S)\, b(i,S,S')\, [S]$$

$$+ \sum_S \sum_{j \geq 1} [e_j]\, v_j [\sigma_{xd}(j,S)\, b_{xd}(j,S,S') + \sigma_i(j,S)\, b_i(j,S,S')]\, [S] \quad . \tag{30}$$

The energy-density changes are monitored for seven modes: ionization, dissociation, electronic excitation, vibrational excitation, radiation, heavy-particle translation and (molecular) rotation, and electron translation. The heavy-particle translational and rotational modes are assumed to be in equilibrium. The energy transfers into the ionization (I), dissociation (D), and electronic excitation (X_e) modes are calculated from

algebraic expressions such as $\sum_{S'} \epsilon \, dS'/dt$ where ϵ represents either the ionization potential of S′, the dissociation energy per atom of S′, or the excitation energy of S′, respectively, and dS'/dt is the rate of increase in S′ resulting from the changes being distinguished. Changes in the remaining energy modes are given by differential equations such as

$$\frac{dM}{dt} = \sum_{S} \sum_{i} \epsilon_M(i,S)\, \varphi(i,t)\, \sigma(i,S)\, [S]\, (1 - \delta_{M,X_v})$$

$$\pm \sum_{S} \sum_{j \geq 1} [e_j]\, v_j \left[e_{Mx}(j,S)\, \sigma_{xd}(j,S) + \epsilon_{Mi}(j,S)\, \sigma_i(j,S) \right] (1 - \delta_{M,X_v})\, [S] \tag{31}$$

where M(eV cm^{-3}) denotes electron translation (E), heavy-particle translation (K), radiation (R), or vibrational excitation (X_v), and the negative sign is used only for M = E. The quantity δ_{M,X_v} is the Kronecker delta. In equation (31),

$$\epsilon_M(i,S) = \sum_{S'} \epsilon_M(i,S,S')\, b(i,S,S')\, (1 - \delta_{M,X_v}) \tag{32a}$$

$$\epsilon_{Mx}(j,S) = \sum_{S'} \epsilon_{Mx}(j,S,S')\, b_{xd}(j,S,S') \tag{32b}$$

$$\epsilon_{Mi}(j,S) = \sum_{S'} \epsilon_{Mi}(j,S,S')\, b_i(j,S,S')\, (1 - \delta_{M,X_v}) \ , \tag{32c}$$

where $\epsilon_M(i,S,S')$, $\epsilon_{Mx}(j,S,S')$, and $\epsilon_{Mi}(j,S,S')$ are determined by examining the energy transformations in each physical process. For M = R, the arguments i and j are omitted.

2.4 Procedure

Calculations of electron-flux spectra and short-time energy and density profiles are made with our E- and F-region computer code in which the above-described procedures are incorporated. The code also computes the solar flux incident on the volume element of interest by calculating, with appropriate use of the Chapman function (see, e.g., Swider and Gardner, 1969), the attenuation of 85 photon groups. Inputs to the code include the time and location of the observations, an atmospheric model, and species and energy densities. Optionally, initial temperatures may be used in place of the electron, heavy-particle, and vibrational energies, from which the initial energies are calculated. The changes in species and energy densities, and then temperatures, are determined by integrating differential equations which include the terms of equations (28) through (31) as well as terms accounting for many other physical and chemical processes. Of these processes, we will mention only those which significantly influence the results discussed herein.

3. PROCESSES AND DATA SOURCES

The physical and chemical processes relevant to energy loss by photoelectrons are described below. Because of the large number of data employed in the modeling calculations, only data sources will be given,

generally. Lists of the detailed data are available from the authors. The cross-section data were averaged over the energy-group widths (Table 1) and were used in this numerical form in the calculations.

3.1 Photoabsorption

The values of the unattenuated solar fluxes in 85 photon groups were taken from Hinteregger (1970). This set excludes any data for repeated spectral intervals of Tables I, II, and III and the first four entries of Table III (Hinteregger, 1970). A slight variation in these data was also used, as discussed below in Section 4.1. The solar photons were absorbed by O, N_2, O_2, and NO in their ground electronic and vibrational states; the range of wavelengths for the solar photons included is 30 to 1306 Å.

Absorption by $O(^3P)$ was limited to the formation of the five atomic oxygen ions listed in Table 2. The cross sections were chosen from the mean of theoretical values (Henry, 1967); these lie between the experimental data (Cairns and Samson, 1965; Comes et al., 1968). Autoionization (Henry, 1968) was not included. Production distribution probabilities, $b(i, S, S')$, were obtained from Henry (1967). Instantaneous radiation by the $O^+(^4P)$ and $O^+(^2P)$ states was assumed; see Table 3.

Absorption by N_2 resulted in the products listed in Table 2. Cross sections were chosen from various sources (Huffman et al., 1963; Samson and Cairns, 1964; Huffman, 1969; Hudson and Carter, 1969; Huffman, 1972). Recent cross-section data (Carter, 1972) of generally

higher resolution and for vibrationally-excited ground-electronic-state N_2 (Cook and McNeal, 1972) were not used in the present calculations but are considered in the discussion of the results (see Section 4.2). Use of intermediate resolution data (Berkowitz and Chupka, 1969) in the range from 700 to 785 Å would not significantly change the adopted cross-section values. For absorption of solar photon groups representing multiplets, the cross sections for lines of the multiplets were averaged, using line strengths (Wiese et al., 1966) as intensity weighting factors, to obtain multiplet cross-sections. In determining the degree of ionization, the cross-section data references given above, as well as other sources (Samson and Cairns, 1964; Cook and Ogawa, 1965), were searched. Where the degree of ionization was less than unity, the formation of the products $N(^4S^\circ)$ and $N(^2D^\circ)$ was regarded as equally probable. At wavelengths above the ionization threshold, predissociation was considered (Hudson and Carter, 1969). The probabilities for ion products, $b(i, S, S')$, were obtained from Blake and Carver (1967) for wavelengths of 580 Å and greater; at smaller wavelengths, the probabilities were assumed to be constant at the values for 580 Å. For the ion products, only the ground vibrational level was assumed to be populated. This is a good approximation for $N_2^+(X\ ^2\Sigma_g^+)$ (Blake and Carver, 1967) and $N_2^+(B\ ^2\Sigma_u^+)$ (Judge and Weissler, 1968), but for $N_2^+(A\ ^2\Pi_u)$, level $v' = 1$ may be significantly populated. Instantaneous radiation by $N_2^+(A\ ^2\Pi_u)$ and $N_2^+(B\ ^2\Sigma_u^+)$ was assumed; see Table 3.

The 11 products of absorption by $O_2(X\ ^3\Sigma_g^-)$ are listed in Table 2. Cross-section data were obtained from various sources (Blake et al., 1966; Cairns and Samson, 1965; Huffman, 1969; Huffman, 1972; Matsunaga and Watanabe, 1967; Samson and Cairns, 1964; Watanabe et al., 1953). Cross sections for multiplet photon-groups were obtained as for N_2. Photoionization coefficients were obtained from Matsunaga and Watanabe (1967). The probabilities $b(i, S, S')$ at wavelengths between the ionization threshold and 580 Å were taken from Blake and Carver (1967); for wavelengths smaller than 580 Å, the probabilities were assumed to be constant at the values for 580 Å. Further, the relation

$$b\left(i, O_2(X\ ^1\Sigma_g^+),\ O_2^+(a\ ^4\Pi_u)\right) = 4\ b\left(i, O_2(X\ ^1\Sigma_g^+),\ O_2^+(A\ ^2\Pi_u)\right) \qquad (33)$$

was assumed; however, see Carlson and Judge (1971). The photodissociation products are not well known (Matsunaga and Watanabe, 1967; Beyer and Welge, 1969; Filseth and Welge, 1969). Below 930 Å, estimates of Matsunaga and Watanabe (1967) and Beyer and Welge (1969) were used; at longer wavelengths, $O(^3P)$ and $O(^1D)$ were regarded as equally probable dissociation products. As in the case of N_2, only the ground vibrational level of ions was assumed to be populated; this is not a good assumption for oxygen, but apparently it is not serious for the results of the present calculation. Instantaneous radiation by $O_2^+(b\ ^4\Sigma_g^-)$, $O_2^+(A\ ^2\Pi_u)$, and $O_2^+(^2\Sigma_g^-)$ was assumed; see Table 3.

The products of absorption by NO were restricted to the list of six in Table 2. Cross-section data were taken from several sources (Cook and Ching, 1965; Sullivan and Holland, 1966; Watanabe, 1958; Watanabe et al., 1967). Resolution of multiplets was not employed for these data as for N_2 and O_2. Ionization coefficients (Cook and Ching, 1965; Watanabe et al., 1967) were arbitrarily set to unity below 580 Å. The product distribution was estimated on the basis of phase-space considerations.

3.2 Collisional excitation and dissociation

The four products of excitation of $O(^3P)$ are given in Table 2; cross-section data for each product state were taken from Henry et al. (1969) and Stone and Zipf (1971). Prompt radiation by $O(3p\ ^3P)$ and $O(3s\ ^3S^\circ)$ was assumed (see Table 3).

See Table 2 for the 10 products considered in excitation of $N_2(X\ ^1\Sigma_g^+)$. For excitation to the $A\ ^3\Sigma_u^+$, $B\ ^3\Pi_g$, $C\ ^3\Pi_u$, and $E\ ^3\Sigma_g^+$ states, data of Borst (1972), Borst et al. (1972), and Jobe et al. (1967) were used but with the recognition of potential difficulties (Shemansky and Broadfoot, 1971a, 1971b). For energies larger than 40 eV, these data were extrapolated by using an E^{-3}-dependence of the cross section, as determined theoretically for triplet states (Chung and Lin, 1972). The cascades $B\ ^3\Pi_g \rightarrow A\ ^3\Sigma_u^+$, $C\ ^3\Pi_u \rightarrow B\ ^3\Pi_g$, and $E\ ^3\Sigma_g^+ \rightarrow A\ ^3\Sigma_u^+$ (however, see Brinkman and Trajmar (1970)), were assumed to occur instantaneously.

The excitation cross-sections to the $a\,^1\Pi_g$ state for $E < 40$ eV (Borst, 1972) and for $2000 \geq E(eV) \geq 100$ (Holland, 1969) are highly compatible; cascade to the $a\,^1\Pi_g$ state is small (Borst, 1972; Ajello, 1970). The radiative decay of the $a\,^1\Pi_g$ state was assumed to occur instantaneously; see Table 3. For excitation to the $c'\,^1\Sigma_u^+$ state, we used cross-section values equal to one half of those of the theoretical calculations (Chung and Lin, 1972) as a compromise between theory and experiment (Aarts and De Heer, 1971), and assumed that the dipole-allowed transition $c'\,^1\Sigma_u^+ \rightarrow X\,^1\Sigma_g^+$ dominates. For excitation to the $a''\,^1\Sigma_g^+$ state, we used the data of Brinkmann and Trajmar (1970); radiative decay to the ground electronic state of N_2 was assumed for the conditions of the observations being modeled, in spite of the facts that the transition is only quadrupole-allowed (Dressler and Lutz, 1967) and other decay modes need to be considered (Brinkmann and Trajmar, 1970). Excitations to the dipole-allowed states $b'\,^1\Sigma_g^+$ and $b\,^1\Pi_u$ were included by using theoretical cross-section curves (Chung and Lin, 1972). For the $b\,^1\Pi_u$ state, 1/10 of the computed cross-section was used since this state is derived from a mixed configuration and the cross section has been computed for only one of two configurations; this is by analogy with the case of the $b'\,^1\Sigma_u^+$ state where taking mixing into account reduces the pure-configuration cross-sections by a factor of 10. The $W\,^3\Delta_u$ state, as well as others, was neglected. However, for the $W\,^3\Delta_u$ state, at least, recent observations (Chutjian et al., 1973)

yield substantially larger cross-sections than predicted. For vibrational excitation of $N_2(X\ ^1\Sigma_g^+)$, we used the data of Chen (1966) for electron energies up to 3.5 eV and other sources for larger energies (Comer and Read, 1971; Pavlovic et al., 1972). Interpolation was required in the energy range between 3.5 and 18 eV.

The dissociative excitation of $N_2(X\ ^1\Sigma_g^+)$, as treated here, leads to the formation of the eight states of atomic nitrogen listed in Table 2, with the product-partner $N(^4S°)$, followed by instantaneous decay as given in Table 3. Cross-section data for each state were taken from several sources (Sheridan et al., 1961; Aarts and De Heer, 1971; Mumma and Zipf, 1971) as compiled by Kieffer (1972), but some extrapolation of the data was required, particularly at the higher electron energies. The treatment of dissociative excitation is also somewhat hampered by lack of knowledge of intermediate states in the excitation processes.

The nine products of excitation and dissociation of $O_2(X\ ^3\Sigma_g^-)$ are given in Table 2. For excitation to the $a\ ^1\Delta_g$ and $b\ ^1\Sigma_g^+$ states, the data (Trajmar et al., 1971) were extended to energies above 45 eV by assuming an E^{-1}-dependence of the cross section. The $c\ ^1\Sigma_u^-$-state excitation data (Trajmar et al., 1972) are limited and were extended by interpolation and extrapolation. The $c\ ^1\Sigma_u^-$ state of O_2, which is not carried as a species in the E- and F-region code, is assumed to dissociate immediately after formation and yield two $O(^3P)$ atoms. For the $B\ ^3\Sigma_u^-$ state, excitation is similar to that

of the $c\ ^1\Sigma_u^-$ state. The data (Trajmar et al., 1972) are limited and estimates (Peterson et al., 1969) have been made; the guessed cross-section curve includes data on excitations at 9.97 and 10.29 eV. Dissociation to $O(^3P) + O(^1D)$ was assumed to be the dominant result of the processes represented by the guessed curve. Data on vibrational excitation is limited (Linder and Schmidt, 1971) to electron energies below 2 eV, although direct excitation to high vibrational levels has been observed (Trajmar et al., 1971). In the present calculation, vibrational excitation was included only for electron energies less than 2 eV.

For dissociative excitation of $O_2(X\ ^3\Sigma_g^-)$ to the $3s\ ^3S°$ state of atomic oxygen (Ajello, 1970; Lawrence, 1970; Mumma and Zipf, 1971; Aarts and De Heer, 1971) and to the $3s\ ^5S°$ state (Wells et al., 1971; Wells and Zipf, 1972), the product partner was taken to be $O(^3P)$. The excited states of atomic oxygen were assumed to radiate instantaneously; see Table 3. Other excited states produced by dissociative excitation of $O_2(X\ ^3\Sigma_g^-)$ (Judge, 1972) were neglected.

For excitation of $O(^3P)$ and excitation and dissociation of $N_2(X\ ^1\Sigma_g^+)$ and $O_2(X\ ^3\Sigma_g^-)$, the probabilities $b_{xd}(k, S, S')$ were determined from the set of cross sections for all processes included in this work.

3.3 Collisional ionization

The total ionization cross-section data for $O(^3P)$ at electron energies greater than 40 eV (Fite and Brackmann, 1959; Rothe et al., 1962)

and below 40 eV (Boksenberg, 1961) as compiled by Kieffer (1969), were combined. The probabilities $b_i(j, S, S')$ were taken from data of Seaton (1959) for electron energies below 250 eV; above 250 eV, the probabilities were taken to be constant at the values corresponding to 250 eV.

For ionization of $N_2(X\ ^1\Sigma_g^+)$, the total cross-section data used were those of Rapp and Englander-Golden (1965). By using these data together with other sources in the case of formation of the $A\ ^2\Pi_u$ state (Shemansky and Broadfoot, 1971b; Holland and Maier, 1973), of the $B\ ^2\Sigma_u^+$ state (Borst and Zipf, 1970), and of the dissociative ionization (Rapp et al., 1965; also see Kieffer and Van Brunt, 1967), we estimated the cross section for production of the $X\ ^2\Sigma_g^+$ state. The data on formation of $B\ ^2\Sigma_u^+$ were multiplied by a factor of 1.12 to account for bands not included in measurements. The radiative decay processes of the $A\ ^2\Pi_u$ and $B\ ^2\Sigma_u^+$ states were assumed to be instantaneous; see Table 3. The $C\ ^2\Sigma_u^+$ and $D\ ^2\Pi_g$ states were neglected. Also, the process of dissociative ionization was greatly simplified by assuming that the products of this process are the neutral and ionized nitrogen atoms in their ground electronic states; note that a reasonably good assumption is that no radiative states of N II are formed in the dissociative ionization process (Aarts and De Heer, 1971).

The six states included in the ionization of $O_2(X\ ^3\Sigma_g^-)$ are listed in Table 2. Total ionization cross-section data were obtained from Rapp and Englander-Golden (1965); data for other states are not extensive in the oxygen

system. For excitation to the $b\,^4\Sigma_g^-$ state, total cross-sections were calculated from the available data (Borst and Zipf, 1970). Adjustments to the data (Skubenich, 1968) for excitation to the $A\,^2\Pi_u$ state were made by (a) multiplying the data by the ratio of the result of Borst and Zipf (1970) to that of Skubenich (1968) for excitation to the $b\,^4\Sigma_g^-$ state and, (b) at energies above the limit of the data, 140 eV, using a constant fraction, 0.35, of calculated cross-sections (Peterson et al., 1969) for the $A\,^2\Pi_u$ state. The fraction 0.35 gave agreement, on the average, between calculated and adjusted data below 140 eV. This fraction was also used to adjust calculated values (Peterson et al., 1969) for excitation of the $a\,^4\Pi_u$ state. The cross sections for excitation to the $^2\Pi_g$ state were obtained as the residual values of the total cross-section data (Rapp and Englander-Golden, 1965) after accounting for other excitations and dissociative ionization (Rapp et al., 1965). The relative values of the $^2\Pi_g$-state excitation cross-sections obtained by this procedure are somewhat larger than calculations predict (Peterson et al., 1969); clearly, additional data are needed, but in the present calculations this lack is not as critical as it is in general, due to the smaller contributions from processes involving molecular oxygen at the altitudes of interest. The recognized prompt radiative transitions following ionization of molecular oxygen are given in Table 3. The treatment of dissociative ionization in molecular oxygen was analogous to that for molecular nitrogen.

For ionization processes, the probabilities $b_i(j, S, S')$ were derived in the same way as for excitation and dissociation processes. The values of $\overline{E}$ for ionization of N_2 and O_2, as used in equation (12), were taken from Opal et al. (1971); $\overline{E}(N_2) = 12.7$, $\overline{E}(O_2) = 17.4$. For O and the dissociative ionization of N_2 and O_2, $\overline{E}$ was estimated by assuming that $\overline{E} \cong I + X$.

3.4 Energy quantities

Energy quantities are required in equations (4), (10), (31), and (32). These were obtained by using established values of the term energies (Table 2) and, for dissociative excitation or ionization, by using the values of the kinetic energy of the heavy-particle fragments. For dissociative ionization of $N_2(X\ ^1\Sigma_g^+)$, roughly 3 eV per atom, when this energy is available, is attributed to the atomic fragments (Kieffer and Van Brunt, 1967; also, see Stockdale and Deleanu, 1973). The same energy per atom was used for dissociative excitation of $N_2(X\ ^1\Sigma_g^+)$ and dissociative ionization of $O_2(X\ ^3\Sigma_g^-)$ in the absence of experimental data. In dissociative excitation of $O_2(X\ ^3\Sigma_g^-)$, roughly 0.5 eV per atom, when available, is attributed to the product atoms (Borst and Zipf, 1971; also, see Freund, 1971; Stockdale and Deleanu, 1973).

The energy quantities for the diatomic products are for the ground vibrational level of the electronic states listed; thus, except for the ground electronic states of N_2 and O_2; no account was taken of the vibrational excitation which occurs in the excitation and ionization of diatomic species.

3.5 Thermal electrons

The thermal-subset electrons undergo some of the above-described processes and others in addition. These interactions are important for their contributions to the electron densities in the low-j groups (see Table 1) and to the total electron density and energy-density changes. The interactions of thermal electrons will be briefly described.

For dissociative recombination of $NO^+(X\ ^1\Sigma^+)$, experimental data (Weller and Biondi, 1968) have been combined with theory (Bardsley, 1970) by using an inverse square-root dependence on the electron temperature, θ. The effect of very recent measurements (Walls and Dunn, 1974) on the dissociative recombination of NO^+, not available when the present calculations were made, is discussed in Section 4.2. Combined data (Kasner and Biondi, 1968; Smith and Goodall, 1968; Mehr and Biondi, 1969; Mahdavi et al., 1971; also, see Cunningham and Hobson, 1972) were used with a temperature dependence of $\theta^{-0.7}$ for dissociative recombination of $O_2^+(X\ ^2\Pi_g)$ and $O_2^+(a\ ^4\Pi_u)$. For $N_2^+(X\ ^2\Sigma_g^+)$, data of Mehr and Biondi (1969) were adjusted to pass through the 300°K-value of Kasner (1967).

Thermal electrons undergo elastic collisions with ions (Banks, 1966) and neutrals (Banks, 1966). (For electron-neutral elastic collisions, the numerical values derived (Valerio, private communication) and used here, from equation (20) together with equations (25), (27), and (29) of Banks (1966), are smaller by a factor of 1.50 than those given in Table 3 of Banks

(1966) for N_2, O_2, and O.) We also included rotational excitation and de-excitation of $N_2(X\ ^1\Sigma_g^+)$ and $O_2(X\ ^3\Sigma_g^-)$ (Dalgarno, 1969); vibrational excitation and de-excitation of $N_2(X\ ^1\Sigma_g^+)$ (Chen, 1966), $O_2(X\ ^3\Sigma_g^-)$ (Linder and Schmidt, 1971), and of $NO(X\ ^2\Pi)$ (Spence and Schulz, 1971); excitation and de-excitation among the ground-configuration terms of neutral and ionized atomic oxygen and nitrogen (Seaton, 1955; Saraph et al., 1966; Czyzak et al., 1967; Moiseiwitsch and Smith, 1968); collisional-radiative recombination with atomic ions of oxygen and nitrogen (Bates et al., 1962; Bates and Kingston, 1964); and cooling of thermal electrons by excitation of the atomic-oxygen ground-term levels. For this fine-structure cooling we used the results of Breig and Lin (1966), following the procedure of Dalgarno and Degges (1968), with account of radiative transfer (Craig and Gille, 1969); however, doubts about the treatment of this mechanism of electron energy loss remain (Takayanagi and Itikawa, 1970).

Transport processes involving (essentially) thermal electrons are discussed in Section 4.2.

3.6 Observational conditions

The observations being modeled were obtained (Hays and Sharp, 1973) on the flight of NASA rocket 13.51 launched February 8, 1971 at White Sands, New Mexico (L 32.°413 N, λ 106.°322 W) at 6:56:18 LT. From more extensive data (Sharp, private communication), we computed zenith angles, including

an approximate correction for the rocket trajectory. The calculations of electron-flux spectra, described in Section 4.1, were made at 180-, 200-, and 250-km altitude, for which the calculated zenith angles are 90.°17, 90.°12, and 89.°95, respectively. Small errors may exist in these values as a result of incomplete data, but these possible errors have negligible effect on the results and discussion (Section 4).

The zenith angles were used in the E- and F-region code to compute the solar flux incident at the altitudes of interest in each of the 85 solar photon groups. Attenuation was attributed to the species $O(^3P)$, $N_2(X\ ^1\Sigma_g^+)$, and $O_2(X\ ^3\Sigma_g^-)$; the densities of these species as well as the temperature of the neutral species were obtained from two atmospheric models: (a) Jacchia (1971), with an exospheric temperature of 1000°K (Hays and Sharp, 1973) and (b) essentially that used by Hays and Sharp (1973) but extended to include N_2. At 120-km altitude, we assumed $[O_2] = 4 \times 10^{10}$ cm^{-3}, $[N_2] = 4 \times 10^{11}$ cm^{-3} (CIRA, 1965), and the ratio $[O]/[O_2] = 3.5$ as in Hays and Sharp (1973). At higher altitudes, we calculated densities and temperatures according to equations (4) and (2) of Walker (1965), with the exospheric temperature $T_\infty = 1000°K$ and $\sigma = 0.01617$ (Jacchia, 1965; Fig. 1, curve 2b).

The initial densities of the ions and electrons required by our E- and F-region code were taken from the flight measurements (Hays and Sharp, 1973). An important minor species is NO; since no measurements

exist for the flight conditions, we used model calculations of the density (Strobel, 1972). Densities of other species included in the chemistry code are unimportant for the present calculations. Initial values of energy densities were calculated from electron temperatures (Hays and Sharp, 1973), neutral-particle temperatures (discussed above), particle densities, and the assumption of equal neutral-particle and vibrational temperatures.

4. RESULTS AND DISCUSSION

The principal results of the calculations reported here are electron-flux spectra at altitudes of 180, 200, and 250 km for the conditions of NASA rocket flight 13.51 on February 8, 1971. These results are compared with measurements of the electron-flux spectra. The effect on the calculations of restrictions imposed by the flight conditions on the rates of change of charged-particle densities is discussed. In addition, photoabsorption and photoelectron interactions are described in terms of formation of species and partition of energy for this flight.

4.1 Electron-flux spectra

The calculated electron-flux spectra at three altitudes are compared with the measured spectra in Fig. 3. The general result is one of good, apparent agreement between the calculated and measured spectra; however, to make such comparisons for spectra at altitudes much above 200 km is questionable. Recent calculations (Mayr et al., 1973) for

energy-deposition profiles show that at 250 km about 1/5 or more of the energy is being deposited over an altitude range greater than the scale height of atomic oxygen. (This result is only indicative of the problem, as the photoelectron spectrum and possibly other conditions of the calculations (Mayr et al., 1973) are not precisely applicable here.) Thus, the circumstances of the agreement at 250 km of the calculated and measured fluxes apparently differ from those at the lower altitudes; nevertheless, this possibility will be put aside in some qualitative discussions below. The complete list of calculated flux values is given in Table 4.

The effect of uncertainties in the input data on the electron-flux spectra has been examined in only a very limited way by varying the atmospheric composition and the solar-flux values. The use of the atmospheric model of Jacchia (1971), on which the calculated electron fluxes in Fig. 3 are based, yields electron-flux values which are smaller by less than 20 per cent than those values obtained by using our extended version of the model of Hays and Sharp (1973). Two solar-flux changes have been examined. If all the solar-flux values are changed by a factor up to 2.5, then the electron-flux values are changed by roughly the same factor in the energy range where thermal electron contributions are negligible. If the solar-flux values recommended by Donnelly and Pope (1973) are adapted to the photon group structure of the present calculations, the electron-flux values differ from those displayed in Fig. 3 by an average of less than 20 per cent at 180 km and by smaller amounts at higher altitudes. The

differences result predominantly from the lower flux values of Donnelly and Pope (1973) in the 100 to 200 Å range.

The uncertainty in the measured values of the electron-flux spectra at 250 km is indicated, for random errors, on Fig. 3. At lower altitudes the counting rates are smaller and the errors are larger (Sharp, private communication); the counting rate is roughly a factor of three lower at 180 km than at 250 km.

There are several prominent features of the measured electron-flux spectra which we discuss in terms of the calculated spectra. The well-known minimum between 2 and 3 eV, resulting from the electron-induced vibrational excitation of N_2, is evident for altitudes of 180 and 200 km (Fig. 3). As the altitude increases, this minimum vanishes since the nitrogen density decreases and the production of electrons with energies in this range increases as the electron density increases. The contribution of thermal electrons to the calculated flux in the 2- to 3-eV range of electron energy is negligible at altitudes of 180 and 200 km, but at 250 km only 8 per cent of the flux is from the high-energy subset of electrons. Two discrepancies may be noted at 180 and 200 km. First, the calculated minimum is much deeper than the measured one and, second, the minimum occurs in the energy range from 2.0 to 2.5 eV in the calculations but in the range from 2.5 to 3.2 eV in the observations. The first discrepancy would not be significantly reduced by accounting for de-excitation of vibrationally-excited nitrogen by high-energy electrons in energy groups below 2 eV (in the

thermal subset of electrons, both excitation and de-excitation are included); inclusion of vibrational de-excitation would increase the fluxes by less than 10 per cent and 20 per cent for the energy ranges from 2.0 to 2.5 eV and from 2.5 to 3.2 eV, respectively. Furthermore, significant error in the total cross-section for vibrational excitation of N_2 seems unlikely, based on recent experiments (Spence et al., 1972). By contrast, the cross sections for excitation of the ground-configuration terms of atomic oxygen are uncertain; these processes are important in the electron energy range in question, and only theoretical values are available. However, doubling or halving the cross section does not change the flux value in the range from 3.2 to 4.0 eV at 180 km (Fig. 3), and doubling the absolute cross-sections while maintaining relative values reduces the depth of the minimum (at 3.2 eV on Fig. 3) by only 10 per cent while increasing the difference in flux values at 4.0 eV. Thus, unless the shape of the theoretical cross-section curve (Henry et al., 1969) is in serious error, the uncertainty in cross-section values for excitation of the ground-configuration terms of atomic oxygen will apparently not account for the first discrepancy.

The second discrepancy, in the energy-location of the minimum, is, from the viewpoint of the calculations, a result of the larger cross-section for vibrationally exciting N_2 in the range from 2.0 to 2.5 eV than in the range from 2.5 to 3.2 eV; a better energy resolution in the calculations might shift the minimum but this has not been determined. A greater

electron temperature would remove the discrepancy but the minimum value required, 1352°K, falls outside the apparent range of scatter of the measured temperatures (Hays and Nagy, 1973) at 180 km.

A possibility for altering both discrepancies simultaneously is the inclusion of a photoelectron flux from the region conjugate to the observation region. The former region is sunlit in the present case. If the conjugate photoelectron flux is as large as that derivable from the measurements of Maier and Rao (1972), then the depth of the calculated minima for 180 and 200 km would be reduced by a factor of two roughly and the minima would be shifted into the 2.5 to 3.2 eV energy range. For larger energies, the qualitative aspects of the electron-flux spectra would be unaltered and flux values would be increased by less than 50 per cent on the average. By contrast, if the conjugate photoelectron flux is as small as that calculated by Nagy and Banks (1970; see also Nagy et al., 1973), then the calculated electron-flux spectra at 180 and 200 km (Fig. 3) would be essentially unaffected.

A plateau occurs between 20 and 30 eV in the electron-flux spectra at 200 and 250 km for both the calculations and observations, as shown in Fig. 3. This plateau is a result of the absorption of the He II solar line at 303.8 Å by O and N_2; Fig. 4 shows a comparison between the electron fluxes with and without the contribution from photoabsorption of the 303.8 Å-He II line. The increased fluxes in the energy group from 20 to

25 eV, shown in Fig. 4, are due principally to the formation of electrons in photoionization processes in which the excited electronic states of the ionized target are produced; for absorbers $O(^3P)$ and $N_2(X\ ^1\Sigma_g^+)$, the principal heavy-particle products are $O^+(^2D^\circ)$, $O^+(^2P^\circ)$, $N_2^+(A\ ^2\Pi_u)$, and $N_2^+(B\ ^2\Sigma_g^+)$. This phenomenon occurs also at 180 km, but there the increased flux from absorption of the 303.8 Å-He II line amounts to a change of only 1.4 per cent at 23 eV and does not form a distinct plateau. With increasing altitude, photoelectron production by absorption of the 303.8 Å-He II line increases significantly and results at 250 km in a relatively larger electron flux in the 23 eV energy bin than in the adjacent bins. Over the range of energies from 14 to 36 eV, the loss-rate coefficient L_j in equation (1) has relative values at 180, 200, and 250 km which change by not more than 15 per cent; the contribution of O dominates in the loss-rate coefficient at these altitudes and this fact is responsible for the small change in the relative values of the loss-rate coefficient in spite of the density changes in O and N_2.

The observations yield only hints of a ledge above 35 eV in the electron-flux spectra; the calculations predict a plateau in the energy range above 35 eV as shown in Fig. 5. This ledge results from the photoabsorption of solar radiation in the wavelength range from about 153 to 205 Å.

This fact is demonstrated in Fig. 5 for three altitudes by comparison of the electron flux calculated with and without the contribution of solar radiation in the stated wavelength interval. According to the data of Hinteregger (1970), which are used here, this wavelength interval is divided at 176 Å into two subintervals for which only the integral flux is presented without further assignment of the radiation to specific sources and wavelengths; however, further assignments can be made (Donnelly and Pope, 1973). Nevertheless, the principal contribution to the ledge is from photoabsorption processes in $O(^3P)$ and $N_2(X\ ^1\Sigma_g^+)$ for which the product ions are in electronically-excited states: $O^+(^2D°)$, $O^+(^2P°)$, $O^+(2s2p^4\ ^4P)$, $N_2^+(A\ ^2\Pi_u)$, and $N_2^+(B\ ^2\Sigma_u^+)$. The decreasing slope of the ledge with increasing altitude is related to the photoabsorption of greater wavelength radiation which produces electrons in the energy group with U_{16} = 36 eV; this contribution increases more rapidly with increasing altitude than does the contribution of photoelectrons to the energy group with U_{17} = 45 eV from photoabsorption of radiation in the wavelength range from 153 to 205 Å.

The energy resolution in the present calculations seems adequate for modeling the observations, as indicated in Fig. 3. Nevertheless, with increased energy resolution, further structure in the electron-flux spectra could be expected to appear and is observed in very recent observations (Mukai and Hirao, 1973). To bring the present calculations

into perspective, the spectrum of the differential photoelectron production rate for the energy interval from 20 to 30 eV is shown in Fig. 6; this spectrum is based on the photoabsorption data described in Section 3.1 but is averaged over 0.2-eV intervals. On the expectation that the structure of this spectrum would be reflected in an electron-flux calculation in which the energy resolution was of the order of tenths of an electron volt, a qualitative comparison of the spectrum with the observations (Mukai and Hirao, 1973) is encouraging for further calculations, in spite of the different conditions of the calculations here and the observations of Mukai and Hirao (1973). A similar qualitative comparison is made by Mukai and Hirao (1973).

4.2 Electron production and loss

While the calculated and observed electron-flux spectra are in reasonable agreement, there is an underlying inconsistency between the production of electrons by photoionization and collisional ionization and the loss of electrons by dissociative recombination. Since the rocket flight (Hays and Sharp, 1973) was at dawn, the net rate of change in electron density is expected to be positive. However, the loss rate exceeds the production rate by factors of 15, 10, and 4.8 at altitudes of 180, 200, and 250 km, respectively. See Table 5. The precise values of these factors depend on our choice of data. For data of one type, such as the unattenuated solar fluxes, an alternate choice of values could reduce these factors

but at the expense of degrading the agreement between the calculated and observed electron-flux spectra. For data of another type, alternate choices would predominantly change only the stated factors. Contributions, including those associated with the latter type of data, which may be important for the inconsistency will now be examined. In the following, "discrepancy" will refer to the positive difference between the electron loss and production rates; while several of the possible contributions can significantly reduce the discrepancy, no definitive explanation for the discrepancy has been found.

A possible source of error in calculating the electron loss rate is the uncertainty in the temperature dependence of the dissociative recombination rate coefficient. This is most likely to be so for the dissociative recombination of NO^+ where the only previously available guide to the correct temperature dependence for ionospheric conditions was theory (Bardsley, 1970). On this basis, in modeling the Hays and Sharp (1973) observations, we assumed the rate coefficient varies as $\theta^{-1/2}$. Very recently, however, ion-storage techniques (Walls and Dunn, 1974) have been used to obtain cross sections for the dissociative recombination of several molecular ions as a function of electron energy. For NO^+, these measurements, when combined with low-temperature experiments (Weller and Biondi, 1968), indicate a stronger dependence of the rate coefficient on the electron temperature than $\theta^{-1/2}$. As an approximate upper limit

to the enhanced dependence, consider a dependence of θ^{-1}. Use of this dependence reduces the electron loss rate by dissociative recombination by roughly 40 per cent. But further theoretical calculations (Michels, 1973) predict a dependence of $\theta^{-0.56}$ for temperatures below 2000°K, so that consistency in knowledge about the temperature dependence of the dissociative recombination rate coefficient is apparently not yet achieved.

Another possible error, uncovered by the work of Gutcheck and Zipf (1973), is that previous experiments (Bardsley and Biondi, 1970) about the dissociative recombination of NO^+, O_2^+, and N_2^+ may have involved vibrationally-excited molecular ions, and this fact may have resulted in derived rate coefficients which are in error. For NO^+, O_2^+, and N_2^+, the rate coefficients most probably decrease as the vibrational energy level of the reacting molecular ion increases (O'Malley, 1969); for dissociative recombination of N_2^+, this is apparently so only for $v \leq 2$ (except in the temperature range between 680 and 3900°K where the rate coefficient for $v = 2$ exceeds that for $v = 0$) (Michels, 1972). Thus, if the experiments (Bardsley and Biondi, 1970) did involve vibrationally-excited molecular ions, correction of the analyses of these experiments would likely yield larger rate coefficients and consequently increase the discrepancies calculated in the modeling of the Hays and Sharp (1973) observations. However, note that in the case of dissociative recombination of O_2^+, shock-tube experiments (Cunningham and Hobson, 1972) and ion-storage experiments

(Walls and Dunn, 1974) are essentially in agreement with afterglow experiments (Weller and Biondi, 1968) and superficial considerations indicate that conditions in the three experiments are not likely to be similar in regard to vibrational excitation of the molecular ions. Further work is needed to establish the occurrence of errors in the rate coefficients as a result of the possibility undercovered by Gutcheck and Zipf (1973), but, at present, this possibility cannot be used to account for the discrepancies in electron production and loss rates under the conditions of the observations (Hays and Sharp, 1973).

In the above argument, the tacit assumption was made that excited vibrational states of molecular ions are not important under quiet ionospheric conditions; this is probably true for NO^+ (Myers, 1973) but has not been investigated for O_2^+ and N_2^+.

A further error source in computing the electron loss rate is associated with uncertainties in the measured densities of electrons and molecular ions; the errors here were not explicitly given (Hays and Sharp, 1973), so further discussion will be left to others.

Contributing to errors in calculation of the rate of change in electron density would be omission of transport processes for electrons and ions. Consider the transport of charged species by ambipolar diffusion, by interaction with neutral winds and electric fields, and by atmospheric expansion. Ideally, the contribution of diffusion (Schunk and Walker, 1973)

could be calculated from the experimental data; however, since this contribution depends principally on the values of the second derivatives of density and temperature with respect to altitude, the calculation is not practical when based on experimental data, as a result of the uncertainties in measured temperatures (Hays and Nagy, 1973) and presumably densities. However, under the restrictions of a monotonic increase in electron density and electron and ion temperatures with increasing altitude and of positive values for the second derivatives of the density and temperatures, one can demonstrate that diffusion is unlikely to account for as much as a third of the discrepancy and, more probably, a considerably smaller fraction. In this estimate, the second derivatives of the density and temperatures had fractional changes with altitude similar to those of the calculated discrepancies over the range from 180 to 250 km.

To determine the contribution of neutral winds to the rate of electron density change is even more difficult than that of diffusion. There were no measurements of winds associated with the rocket flight (Hays and Sharp, 1973) and appropriate calculations of the winds have not been made. However, models of neutral winds (Kohl and King, 1967; Sterling et al., 1969; Strobel and McElroy, 1970) indicate that during the night, a wind component results in flow from north to south and thereby causes an upward drift of ionization along geomagnetic field lines, whereas during the day, the wind direction and ionization drift are reversed. The models also

indicate that during the time of the rocket flight, the north-south component of the wind had just or was about to change direction, with the consequence that velocities were of the order of tens of meters per second rather than of the order of hundreds of meters per second which may occur at other times. Furthermore, if neutral winds are to contribute to removing the discrepancies of the present calculations, a positive value of the rate of electron density change must obtain. On the basis of these considerations, an estimate indicates that the interaction of neutral winds with charged species accounts for less than 20 per cent of the discrepancies.

The contribution of electric fields is also probably unimportant, as calculations have demonstrated (Rüster, 1971) that neutral winds are more important than electric fields in their effect on the behavior of the F region.

Finally, the expansion of the atmosphere (Sterling et al., 1969), which has a nearly maximum rate during the time of the rocket flight, results in an electron loss rate which is less than 1.5 per cent of the discrepancies.

Accounting for electrons from the region conjugate to the observation region (see Section 4.1) could increase the calculated electron production rate and thus decrease the discrepancies. But, conjugate electron fluxes based on recent measurements at the altitudes of interest (Maier and Rao, 1972) or on a combination of measurements and calculations (Nagy and Banks, 1970; Nagy et al., 1973) would reduce the discrepancies by less than 6 per cent.

Errors in calculating the photoelectron production rate can arise from certain aspects of the present treatment of the photoionization processes and from omission of processes. (Below, "photoelectron production" will refer to formation of electrons by only photoionization.) In certain spectral intervals, average absorption cross-sections were used where there is significant variation of the cross section with wavelength. The use of average cross-sections leads to errors in calculating the incident solar flux at the altitudes of interest and to an additional error in calculating the amount of photoabsorption. At photon energies $h\nu$ less than the thresholds $h\nu_i(N_2)$ and $h\nu_i(O_2)$ for ionization of N_2 and O_2, photoionization of O_2 and NO will be treated incorrectly; at $h\nu > [h\nu_i(N_2),\ h\nu_i(O_2)]$, the amount of photoionization of N_2 and O_2 will be in error. The effect of using average absorption cross-sections was examined for N_2 at $h\nu(eV) < h\nu_i(N_2) + 1$ and for O_2 at $h\nu(eV) < h\nu_i(O_2) + 1$ by recomputing the photoionization of N_2, O_2, and NO with more accurate cross-section values or selected cross-section values which maximized the amount of photoionization in the spectral interval of averaging. For $h\nu < [h\nu_i(N_2),\ h\nu_i(O_2)]$, the increase in photoionization of O_2 and NO was less than 25 per cent of the presently computed rate of photoelectron production at 180 km under the conditions of the observations (Hays and Sharp, 1973) and consequently less than 1 per cent of the discrepancy between electron loss and production rates. For $h\nu > [h\nu_i(N_2),\ h\nu_i(O_2)]$, the change in the amount of photoionization between 180 and 250 km was negligible with respect to the discrepancies.

The photoelectron production rate may be increased by including vibrationally-excited absorbers with smaller ionization thresholds than for unexcited absorbers. We estimated the effect of including vibrationally-excited N_2 in the photoabsorption processes by (a) using absorption data for vibrationally-excited N_2 (Cook and McNeal, 1972), (b) assuming a vibrational temperature of 2500°K, which is larger than expected (Breig et al., 1973), and (c) omitting attenuation of the solar radiation. The increase in the photoelectron production rate by N_2 absorbing radiation in the range from 796 to 842 Å was less than 12 per cent of the rate without considering vibrationally-excited N_2 and was negligible in comparison with the discrepancies. For vibrationally-excited O_2, no photoionization data are available in the range from 1027 to 1080 Å; however, for an assumed vibrational temperature of 2500°K, the contributions of vibrationally-excited O_2 to the photoelectron production rate would be negligible in comparison with the discrepancies, provided the absorption cross-sections are less than about 10^{-17} cm^2. But for computing the photoelectron production rate, these contributions could be non-negligible provided the photoionization cross-section of vibrationally-excited O_2 is effectively 5×10^{-18} cm^2 or larger for the C II and O VI multiplets in the vicinity of 1032 and 1037 Å, and the solar flux values of Donnelly and Pope (1973) are essentially correct.

The effect of rotationally-excited N_2 and O_2 is also negligible with regard to the electron production and loss discrepancies.

Certain absorptions by atomic oxygen (Huffman and Larrabee, 1968) were neglected in our calculations. Of these absorptions, only that of the H Lyman-beta line by $O(^3P_2)$ is non-negligible. On the basis of the ratio of the Lyman-alpha flux to the Lyman-beta flux observed at approximately 185 km (Detwiler et al., 1961), the attenuation of the Lyman-beta flux in our electron-flux calculations is in error to the extent of overestimating the photoelectron production rate by about 4 per cent; this is small compared with the discrepancies at 180 km. At higher altitudes this error in attenuation is even less important.

The uncertainty in [NO] could significantly affect the discrepancy at 180 km, listed in Table 5, since the photoionization of NO accounts for about 25 per cent of the photoelectrons formed at 180 km. The density of NO was based only on calculations (Strobel, 1972).

Under other conditions, Swartz and Nisbet (1973) have found a discrepancy similar to the one discussed above and Roble and Dickinson (1973) have found a related one. These investigators suggest that underestimation of solar fluxes might account for the discrepancies; this possibility appears less tenable in the present calculations for the reason stated at the beginning of this section. Increases in the solar EUV flux values by factors of two to three as proposed (Swartz and Nisbet, 1973; Roble and

Dickinson, 1973) would leave the present calculation with a still significant discrepancy between electron production and loss.

4.3 Species and energy partitioning

The species formation and the transformation of energy associated with photoabsorption and the subsequent interactions of the high-energy electrons have been compiled for the conditions of the observations. As stated in Section 2.3, this compilation excludes changes involving ambient electrons, chemical reactions, and transport of energy and species. In Table 6, the relative formation rates for species are listed when these rates equal or exceed 0.01 of the total; the total, absolute rates are 273, 378, and 535 cm^{-3} sec^{-1} for altitudes of 180, 200, and 250 km, respectively. Several of these values are noteworthy. The large fractional contribution for $O(^1D)$ arises from electron collisional excitation. The fractional contribution of $O(3s\ ^3P)$ seems rather large in view of its excitation energy but this is due to a combination of two factors: a sharply peaked cross-section-versus-energy curve for formation of $O(3s\ ^3P)$ by electron impact in the energy range between 12 and 32 eV (Stone and Zipf, 1971) with a large maximum cross-section and a fractional increase in electron flux with increasing altitude which is largest in the same energy range. For formation of vibrationally excited nitrogen, $N_2(X\ ^1\Sigma_g^+)^{v'}$, the maximum as a function of altitude in the relative rates follows from the maximum in

the product of densities for electrons and nitrogen molecules, the electron density increasing and the nitrogen density decreasing with altitude. The formation of $N_2(A\ ^2\Sigma^+)$ is predominantly by absorption of radiation with energy less than the ionization threshold for nitrogen as treated here. A more careful treatment of this process would undoubtedly reduce the listed relative rates of formation and increase those of atomic nitrogen species.

The energy partitioning is shown in Table 7 in terms of the relative rates of change in the seven energy modes. See Section 2.3. For each altitude, the first column shows the partitioning immediately following photoabsorption (PA) and the second column shows the partitioning when the steady-state in the high-energy electron subset has been established (SS), i.e., after this subset has excited, dissociated and ionized the target species.

5. CONCLUSIONS

Electron-flux spectra, calculated for 180-, 200-, and 250-km altitude, are in reasonable agreement with electron-flux spectra measured for dawn conditions in midlatitude (Hays and Sharp, 1973). The agreement indicates that the processes and data employed are sufficient for calculations with spectral energy resolution of approximately 20 per cent. Certain prominent spectral features are shown to be associated with photoabsorption processes in which electronically-excited ions are formed;

greater spectral resolution in both calculations and observations is needed to probe more deeply into these spectral features.

The loss rate of electrons by dissociative recombination, based on measured electron and ion densities, exceeds the calculated rate of forming electrons by photoionization and collisional ionization. This discrepancy decreases with increasing altitude. No definitive explanation for the discrepancy was found, although a number of processes associated with photoabsorption, particle transport, and data errors were examined.

Acknowledgements — This research was supported by the Defense Advanced Research Projects Agency of the Department of Defense and was monitored by the Office of Naval Research under Contract No. N00014-72-C-0292. The authors gratefully acknowledge discussions with Dr. W. E. Sharp of the Department of Aerospace Engineering, Meteorology and Oceanography, University of Michigan.

REFERENCES

Aarts J. F. M. and De Heer F. J.	1971	Physica 52, 45.
Ajello J. M.	1970	J. chem. Phys. 53, 1156.
Anderson R.	1971	Atomic Data 3, 227
Banks P.	1966	Planet. Space Sci. 14, 1085.
Bardsley J. N.	1970	Phys. Rev. A2, 1359.
Bardsley J. N. and Biondi M. A.	1970	Advances in Atomic and Molecular Physics (Edited by D. R. Bates and I. Esterman) 6, p. 1. Academic Press, New York.
Bates D. R. and Kingston A. E.	1964	Proc. phys. Soc. 83, 43.
Bates D. R., Kingston A. E. and McWhirter R. W. P.	1962	Proc. R. Soc. A270, 155.
Berkowitz J. and Chupka W. A.	1969	J. chem. Phys. 51, 2341.
Beyer K. D. and Welge K. H.	1969	J. chem. Phys. 51, 5323.
Blake A. J. and Carver J. H.	1967	J. chem. Phys. 47, 1038.
Blake A. J., Carver J. H. and Haddad G. N.	1966	J. Quant. Spectrosc. Rad. Trans. 6, 451.
Borst W. L.	1972	Phys. Rev. A5, 648.
Borst W. L., Wells W. C. and Zipf E. C.	1972	Phys. Rev. A5, 1744.

Borst W. L. and Zipf E. C.	1970	Phys. Rev. A1, 1410.
Borst W. L. and Zipf E. C.	1971	Phys. Rev. A4, 153.
Breig E. L., Brennan M. E. and McNeal R. J.	1973	J. geophys. Res. 78, 1225.
Breig E. L. and Lin C. C.	1966	Phys. Rev. 151, 67.
Brinkman R. T. and Trajmar S.	1970	Annls Géophys. 26, 201.
Cairns R. B. and Samson J. A. R.	1965	Phys. Rev. 139, A1403.
Carlson R. W. and Judge D. L.	1971	J. chem. Phys. 54, 1832.
Carter V. L.	1972	J. chem. Phys. 56, 4195.
Chung S. and Lin C. C.	1972	Phys. Rev. A6, 988.
Chutjian A., Cartwright D. C. and Trajmar S.	1973	Phys. Rev. Letts 30, 195.
CIRA	1965	COSPAR International Reference Atmosphere. North-Holland, Amsterdam.
Comer J. and Read F. H.	1971	J. Phys. B4, 1055.
Comes F. J., Speier F. and Elzer A.	1968	Z. Naturforsch. 23a, 125.
Cook G. R. and McNeal R. J.	1972	J. chem. Phys. 56, 1388.
Cook G. R. and Ogawa M.	1965	Can. J. Phys. 43, 256.
Craig R. A. and Gille J. C.	1969	J. atmos. Sci. 26, 205.

Cunningham A. J. and Hobson R. M.	1972	J. Phys. B5, 2320.
Czyzak S. J., Krueger T. K. and Saraph H. E.	1967	Proc. phys. Soc. 92, 1146.
Dalgarno A.	1968	Advances in Atomic and Molecular Physics (Edited by D. R. Bates and I. Esterman) 4, p. 381. Academic Press, New York.
Dalgarno A.	1969	Can. J. Chem. 47, 1723.
Dalgarno A. and Degges T. C.	1968	Planet. Space Sci. 16, 125.
Detwiler C. R., Garrett D. L. and Purcell J. D.	1961	Annls Géophys. 17, 263.
Dressler K. and Lutz B. L.	1967	Phys. Rev. Letts 19, 1219.
Filseth S. V. and Welge K. H.	1969	J. chem. Phys. 51, 839.
Fite W. L. and Brackmann R. T.	1959	Phys. Rev. 113, 815.
Freund R. S.	1971	J. chem. Phys. 54, 3125.
Gutcheck R. A. and Zipf E. C.	1973	J. geophys. Res. 78, 5429.
Hays P. B. and Nagy A. F.	1973	Planet. Space Sci. 21, 1301.
Hays P. B. and Sharp W. E.	1973	J. geophys. Res. 78, 1153.
Henry R. J. W.	1967	Planet. Space Sci. 15, 1747.
Henry R. J. W.	1968	Planet. Space Sci. 16, 1503.

Henry R. J. W., Burke P. G. and Sinfailam A. L.	1969	Phys. Rev. 178, 218.
Herzberg G.	1950	Molecular Spectra and Molecular Structure I. Spectra of Diatomic Molecules. Van Nostrand, Princeton, N. J.
Hinteregger H. E.	1970	Annls Géophys. 26, 547.
Holland R. F.	1969	J. chem. Phys. 51, 3940.
Holland R. F. and Maier II W. B.	1973	J. chem. Phys. 58, 2672.
Hudson R. D. and Carter V. L.	1969	J. geophys. Res. 74, 393.
Huffman R. E.	1969	Can. J. Chem. 47, 1823.
Huffman R. E. and Larrabee J. C.	1968	J. geophys. Res. 73, 7419.
Huffman R. E., Tanaka Y. and Larrabee J. C.	1963	J. chem. Phys. 39, 910.
Jacchia L. G.	1965	Smithsonian Contributions to Astrophysics 8, 215.
Jobe J. D., Sharpton F. A. and St. John R. M.	1967	J. opt. Soc. Am. 57, 106.
Judge D. L. and Weissler G. L.	1968	J. chem. Phys. 48, 4590.

Judge R. J. R.	1972	Planet. Space Sci. 20, 2081.
Kasner W. H.	1967	Phys. Rev. 164, 194.
Kasner W. H. and Biondi M. A.	1968	Phys. Rev. 174, 139.
Kieffer L. J.	1969	Atomic Data 1, 19.
Kieffer L. J. and Van Brunt R. J.	1967	J. chem. Phys. 46, 2728.
Kohl H. and King J. W.	1967	J. Atmos. Terr. Phys. 29, 1045.
Krinberg I. A.	1973	Planet. Space Sci. 21, 523.
Lawrence G. M.	1970	Phys. Rev. A2, 397.
Linder F. and Schmidt H.	1971	Z. Naturforsch. 26a, 1617.
Mahdavi M. R., Hasted J. B. and Nakshbandi M. M.	1971	J. Phys. B4, 1726.
Maier E. J. and Rao B. C. N.	1972	J. Atmos. Terr. Phys. 34, 689.
Matsunaga F. M. and Watanabe K.	1967	Sci. Light 16, 31.
Mayr H. G., Fontheim E. G., and Robertson S. C.	1973	Radio Sci. 8, 47.
Mehr F. J. and Biondi M. A.	1969	Phys. Rev. 181, 264.
Michels H. H.	1973	Abstracts of the Eighth International Conference on the Physics of Electronic and Atomic Collisions, p. 891. Institute of Physics, Beograd.

Moiseiwitsch B. L. and Smith S. J.	1968	Rev. Mod. Phys. 40, 238.
Mumma M. J. and Zipf E. C.	1971	J. chem. Phys. 55, 1661.
Mukai T. and Hirao K.	1973	J. geophys. Res. 78, 8395.
Myers B. F.	1973	J. Atmos. Terr. Phys. 35, 1903.
Nagy A. F. and Banks P. M.	1970	J. geophys. Res. 75, 6260.
Nagy A. F., Winningham J. D. and Banks P. M.	1973	J. Atmos. Terr. Phys. 35, 2289.
O'Malley T. F.	1969	Phys. Rev. 185, 101.
Opal C. B., Peterson W. K. and Beaty E. C.	1971	J. chem. Phys. 55, 4100.
Pavlovic Z., Boness M. J. W., Herzenberg A. and Schulz G. J.	1972	Phys. Rev. A6, 676.
Peterson L. R., Prasad S. S. and Green A. E. S.	1969	Can. J. Chem. 47, 1774.
Rapp D. and Englander-Golden P.	1965	J. chem. Phys. 43, 1464.
Rapp D., Englander-Golden P. and Briglia D. D.	1965	J. chem. Phys. 42, 4081.
Roble R. G. and Dickinson R. E.	1973	J. geophys. Res. 78, 249.

Rothe E. W., Neynaber R., Marino L. L. and Trujillo S. M. 1962 Phys. Rev. 125, 582.

Rüster R. 1971 J. Atmos. Terr. Phys. 33, 275.

Samson J. A. R. and Cairns R. B. 1964 J. geophys. Res. 69, 4583.

Saraph H. E., Seaton M. J. and Shemming J. 1966 Proc. phys. Soc. 89, 27.

Schunk R. W. and Hays P. B. 1971 Planet. Space Sci. 19, 113.

Schunk R. W. and Walker J. C. G. 1973 Planet. Space Sci. 21, 526.

Seaton M. J. 1955 The Airglow and the Aurorae (Edited by E. B. Armstrong and A. Dalgarno), p. 289. Pergamon, London.

Seaton M. J. 1959 Phys. Rev. 113, 814.

Shemansky D. E. and Broadfoot A. L. 1971a J. Quant. Spectrosc. Rad. Trans. 11, 1385.

Shemansky D. E. and Broadfoot A. L. 1971b J. Quant. Spectrosc. Rad. Trans. 11, 1401.

Sheridan W. F., Oldenberg O. and Carleton N. P.	1961	Abstracts of the Second International Conference on the Physics of Electronic and Atomic Collisions, p. 159. W. A. Benjamin, New York.
Skubenich V. V.	1968	Opt. Spectrosc. 25, 90.
Smith D. and Goodall C. V.	1968	Planet. Space Sci. 16, 1177.
Spence D., Mauer J. L. and Schulz G. J.	1972	J. chem. Phys. 57, 5516.
Spence D. and Schulz G. J.	1971	Phys. Rev. A3, 1968.
Sterling D. L., Hanson W. B., Moffett R. J. and Baxter R. G.	1969	Radio Sci. 4, 1005.
Stockdale J. A. D. and Deleanu L.	1973	Chem. Phys. Letts 22, 204.
Stone E. J. and Zipf E. C.	1971	Phys. Rev. A4, 610.
Strobel D. F.	1972	Radio Sci. 7, 1.
Strobel D. F. and McElroy M. B.	1970	Planet. Space Sci. 18, 1181.
Swartz W. E. and Nisbet J. S.	1973	J. geophys. Res. 78, 5640.
Swider W., Jr. and Gardner M. E.	1969	Applied Optics 8, 725.

Takayanagi K. and Itikawa Y. 1970 Space Sci. Rev. 11, 380.

Trajmar S., Cartwright D. C. and Williams W. 1971 Phys. Rev. A4, 1482.

Trajmar S., Williams W. and Kuppermann A. 1972 J. chem. Phys. 56, 3759.

Walker J. C. G. 1965 J. atmos. Sci. 22, 462.

Walls F. L. and Dunn G. H. 1974 Bull. Am. phys. Soc. 19, 150.

Watanabe K. 1958 Advances in Geophysics (Edited by H. E. Landsberg and J. Van Miegham), p. 153. Academic Press, New York.

Watanabe K., Matsunaga F. M. and Sakai H. 1967 Applied Optics 6, 391.

Weller C. S. and Biondi M. A. 1968 Phys. Rev. 172, 198.

Wells W. C., Borst W. L. and Zipf E. C. 1971 Chem. Phys. Letts 12, 288.

Wells W. C. and Zipf E. C. 1972 Trans. Am. Geophys. Un. 53, 459.

Wiese W. L., Smith M. W. and Glennon B. M. 1966 National Standard Reference Data Series, Number 4 (National Bureau of Standards) U. S. Government Printing Office, Washington, D. C.

Reference is also made to the following unpublished material:

Boksenberg A.	1961	Ph. D. Thesis, Univ. of London.
Chen J. C. Y.	1966	JILA Rep. No. 70, University of Colorado, Boulder, Colo.
Cook G. R. and Ching B. K.	1965	Aerospace Corp. Rep. TDR-469(9260-01)-4. El Segundo, Calif.
Donnelly R. F. and Pope J. H.	1973	National Oceanic and Atmospheric Administration Rep. ERL 276-SEL25. Boulder, Colo.
Huffman R. E.	1972	Defense Nuclear Agency Rep. 1948H, Washington, D. C.
Jacchia L. G.	1971	Smithsonian Astrophysical Observatory Special Rep. No. 332. Cambridge, Mass.
Kieffer L. J.	1972	JILA Information Center Rep. No. 12. Univ. of Colorado, Boulder, Colo.
Michels H. H.	1972	Abstracts of the Third International Conference on Atomic Physics, p. 173. Boulder, Colo.
Sullivan J. O. and Holland A. C.	1966	NASA Rep. No. CR-371. Washington, D. C.

Watanabe K., Zelikoff M. and Inn E. C. Y. 1953 Air Force Cambridge Research Center Tech. Rpt. No. 53-23. Bedford, Mass.

Table 1. Energy groups used in treating electron energy loss processes

Group No., * j	U_j†, eV	ΔU_j†, eV	$W_j = \sum_{i=0}^{j} \Delta U_i$†
0	0.5‡	1.0	1.0
1	1.1	0.25	1.25
2	1.4	0.35	1.6
3	1.8	0.4	2.0
4	2.3	0.5	2.5
5	2.9	0.7	3.2
6	3.6	0.8	4.0
7	4.5	1.0	5.0
8	5.7	1.4	6.4
9	7.2	1.6	8.0
10	9.0	2.0	10.0
11-20	$10\ U_{j-10}$	$10\ \Delta U_{j-10}$	$10\ W_{j-10}$
21-30	$100\ U_{j-20}$	$100\ \Delta U_{j-20}$	$100\ W_{j-20}$

*The high-energy subset of electrons are those electrons in group j=1 to 30.

†U_j is the characteristic energy of group j; ΔU_j is the width of group j; W_j is the upper-edge energy of group j.

‡When it is necessary to adopt probabilities for an electron to enter both the thermal subset and group 1, a characteristic energy of 0.5 eV is assigned to the lower-energy electron, which energy is then added to the total thermal-electron energy.

Table 2. Species and Energy Quantities

Product	Target $O(^3P)$	Target $O_2(X^3\Sigma_g^-)$	Target $NO(X^2\Pi)$	Energy, eV	Product	Target $N_2(X^1\Sigma_g^+)$	Target $NO(X^2\Pi)$	Energy, eV
$O(^3P)$		a,xd,i*	a	2.56†	$N(^4S^\circ)$	a,i	a	4.88†
$O(^1D)$	xd	a,xd	a	1.96	$N(^2D^\circ)$	a	a	2.37
$O(^1S)$	xd	a		4.17	$N(^2P^\circ)$		a	3.56
$O(3s\ ^5S^\circ)$		xd		9.14	$N(3s\ ^4P)$	xd		10.33
$O(3s\ ^3S^\circ)$	xd	a,xd		9.52	$N(3s\ ^2P)$	xd		10.67
$O(3p\ ^5P)$		a		10.74	$N(2p^4\ ^4P)$	xd		10.93
$O(3p\ ^3P)$	xd	a		10.99	$N(3p\ ^4D^\circ)$	xd		11.70
$O^+(^4S^\circ)$	a,i	i		13.62	$N(3p\ ^4P^\circ)$	xd		11.78
$O^+(^2D^\circ)$	a,i			16.93	$N(3s'\ ^2D)$	xd		12.34
$O^+(^2P^\circ)$	a,i			18.62	$N(4s\ ^2P)$	xd		12.86
$O^+(2s2p^4\ ^4P)$	a			28.49	$N(3d\ ^2D)$	xd		13.02
$O^+(2s2p^4\ ^2P)$	a			39.98	$N_2(X^1\Sigma_g^+, v>0)$	xd		-
$O_2(X^3\Sigma_g^-, v>0)$		xd		-	$N_2(A^3\Sigma_u^+)$	a,xd		6.17
$O_2(a\ ^1\Delta_g)$		xd		0.98	$N_2(B^3\Pi_g)$	xd		7.35
$O_2(b\ ^1\Sigma_g^+)$		xd		1.63	$N_2(a\ ^1\Pi_g)$	xd		8.55
$O_2(c\ ^1\Sigma_u^-)$		xd		4.05	$N_2(C\ ^3\Pi_u)$	xd		11.02
$O_2(B\ ^2\Sigma_u^-)$		xd		6.12	$N_2(E\ ^3\Sigma_g^+)$	xd		11.87
$O_2^+(X\ ^2\Pi_g)$		a,i		12.06	$N_2(a'\ ^1\Sigma_g^+)$	xd		12.28
$O_2^+(a\ ^4\Pi_u)$		a,i		16.10	$N_2(b\ ^1\Pi_u)$	xd		12.57
$O_2^+(A\ ^2\Pi_u)$		a,i		16.81	$N_2(c'\ ^1\Sigma_u^+)$	xd		12.93
$O_2^+(b\ ^4\Sigma_g^-)$		a,i		18.2	$N_2(b'\ ^1\Sigma_u^+)$	xd		13.21
$O_2^+(^2\Sigma_g^-)$		a		20.0	$N^+(^3P)$	i		14.53
					$N_2^+(X\ ^2\Sigma_g^+)$	a,i		15.58
					$N_2^+(A\ ^2\Pi_u)$	a,i		16.58
					$N_2^+(B\ ^2\Sigma_u^+)$	a,i		18.75
					$NO^+(X\ ^1\Sigma^+)$		a	10.20

*a ≡ photoabsorption; xd ≡ collisional excitation and dissociation; i ≡ collisional ionization.

†The energy reference for all monatomic products is the energy of $O(^3P)$ or $N(^4S)$ except for these latter; for diatomic products as well as $O(^3P)$ or $N(^4S^\circ)$, the energy reference is provided by $O_2(X\ ^3\Sigma_g^-) + N_2(X\ ^1\Sigma_g^+)$ Energy differences among levels of $O(^3P_{0,1,2})$ have been neglected except in the treatment of fine-structure cooling.

Table 3. Radiative Processes Regarded as Instantaneous

Transition	Initiating Process*	τ, sec†	$\epsilon_R(S,S')$, eV
$O(3s\ ^5S^\circ) \rightarrow O(^3P) + h\nu$	xd $O_2(X\ ^3\Sigma_g^+)$	6(-4)‡	9.14
$O(3s\ ^3S^\circ) \rightarrow O(^3P) + h\nu$	a, xd $O_2(X\ ^3\Sigma_g^+)$, xd $O(^3P)$	2.6(-9)	9.52
$O(3p\ ^5P) \rightarrow O(3s\ ^5S^\circ) + h\nu$	a $O_2(X\ ^3\Sigma_g^+)$	2.9(-8)	1.60
$O(3p\ ^3P) \rightarrow O(3s\ ^3S^\circ) + h\nu$	a $O_2(X\ ^3\Sigma_g^+)$, xd $O(^3P)$	3.6(-8)	1.47
$O^+(2s2p^4\ ^4P) \rightarrow O^+(^4S^\circ) + h\nu$	a $O(^3P)$	7.1(-10)	14.87
$O^+(2s2p^4\ ^2P) \rightarrow O^+(^2D^\circ) + h\nu$	a $O(^3P)$	5.6(-10)	23.05
$O_2^+(A\ ^2\Pi_u) \rightarrow O_2^+(X\ ^2\Pi_g) + h\nu$	a, i $O_2(X\ ^3\Sigma_g^-)$	~6.7(-7)	4.75
$O_2^+(b\ ^4\Sigma_g^-) \rightarrow O_2^+(a\ ^4\Pi_u) + h\nu$	a, i $O_2(X\ ^3\Sigma_g^-)$	≤1.2(-6)	2.1
$O_2^+(^2\Sigma_g^-) \rightarrow O_2^+(A\ ^2\Pi_u) + h\nu$	a $O_2(X\ ^3\Sigma_g^-)$		3.19
$N(3s\ ^4P) \rightarrow N(2p^3\ ^4S^\circ) + h\nu$	i $N_2(^1\Sigma_g^+)$	4.3(-9)	10.33
$N(3s\ ^2P) \rightarrow N(2p^3\ ^2D^\circ) + h\nu$	i $N_2(^1\Sigma_g^+)$	1.8(-9)	8.30
$N(3s\ ^2P) \rightarrow N(2p^3\ ^2P^\circ) + h\nu$	i $N_2(^1\Sigma_g^+)$	5.0(-9)	7.11
$N(2p^4\ ^4P) \rightarrow N(2p^3\ ^4S^\circ) + h\nu$	i $N_2(^1\Sigma_g^+)$	1.9(-9)	10.93
$N(3p\ ^4D^\circ) \rightarrow N(3s\ ^4P) + h\nu$	i $N_2(^1\Sigma_g^+)$	5.3(-8)	1.37
$N(3p\ ^4P^\circ) \rightarrow N(3s\ ^4P) + h\nu$	i $N_2(^1\Sigma_g^+)$	4.4(-8)	1.45
$N(3s'\ ^2D) \rightarrow N(2p^3\ ^2D^\circ) + h\nu$	i $N_2(^1\Sigma_g^+)$	2.2(-9)	9.97
$N(4s\ ^2P) \rightarrow N(2p^3\ ^2D^\circ) + h\nu$	i $N_2(^1\Sigma_g^+)$	9.1(-9)	10.49
$N(3d\ ^2D) \rightarrow N(2p^3\ ^2D^\circ) + h\nu$	i $N_2(^1\Sigma_g^+)$	2.1(-8)	10.65
$N_2(B\ ^3\Pi_g) \rightarrow N_2(A\ ^3\Sigma_u^+) + h\nu$	xd $N_2(X\ ^1\Sigma_g^+)$	~8. (-6)	1.18
$N_2(a\ ^1\Pi_g) \rightarrow N_2(X\ ^1\Sigma_g^+) + h\nu$	xd $N_2(X\ ^1\Sigma_g^+)$	<2. (-4)	8.55
$N_2(C\ ^3\Pi_u) \rightarrow N_2(B\ ^3\Pi_g) + h\nu$	xd $N_2(X\ ^1\Sigma_g^+)$	≤6. (-8)	3.67
$N_2(E\ ^3\Sigma_g^+) \rightarrow N_2(A\ ^3\Sigma_u^+) + h\nu$	xd $N_2(X\ ^1\Sigma_g^+)$	≤3. (-4)	5.70
$N_2(a'\ ^1\Sigma_g^+) \rightarrow N_2(X\ ^1\Sigma_g^+) + h\nu$	xd $N_2(X\ ^1\Sigma_g^+)$	1§	12.28
$N_2(b\ ^1\Pi_u) \rightarrow N_2(X\ ^1\Sigma_g^+) + h\nu$	xd $N_2(X\ ^1\Sigma_g^+)$	da‖	12.57
$N_2(c'\ ^1\Sigma_u^+) \rightarrow N_2(X\ ^1\Sigma_g^+) + h\nu$	xd $N_2(X\ ^1\Sigma_g^+)$	da	12.93
$N_2(b'\ ^1\Sigma_u^+) \rightarrow N_2(X\ ^1\Sigma_g^+) + h\nu$	xd $N_2(X\ ^1\Sigma_g^+)$	da	13.21
$N_2^+(A\ ^2\Pi_u) \rightarrow N_2^+(X\ ^2\Sigma_g^+) + h\nu$	a, i $N_2(X\ ^1\Sigma_g^+)$	~1.2(-5)	1.0
$N_2^+(B\ ^2\Sigma_u^+) \rightarrow N_2^+(X\ ^2\Sigma_g^+) + h\nu$	a, i $N_2(X\ ^1\Sigma_g^+)$	≤7. (-5)	3.17

*a ≡ photoabsorption; xd ≡ collisional excitation and dissociation; i ≡ collisional ionization.

†Monatomic radiative lifetimes from Wiese et al. (1966); diatomic radiative lifetimes from Anderson (1971).

‡Decadic exponents are enclosed in parentheses.

§Estimate; see Herzberg (1950).

‖da ≡ dipole allowed, Chung and Lin (1972).

Table 4. Calculated Electron Flux for Energy Groups

U_j, eV	Flux, $(cm^2\ sec\ eV)^{-1}$		
	180 km	200 km	250 km
1.1	3.13(9)†	2.11(10)	7.46(11)
1.4	4.26(8)	2.85(9)	1.78(11)
1.8	6.38(7)	3.17(8)	2.71(10)
2.3	1.07(7)	5.10(7)	2.09(9)
2.9	1.27(7)	5.45(7)	3.69(8)
3.6	4.27(7)	1.24(8)	2.54(8)
4.5	3.36(7)	9.90(7)	2.50(8)
5.7	2.52(7)	7.63(7)	2.20(8)
7.2	1.46(7)	4.90(7)	1.91(8)
9.0	4.59(6)	1.70(7)	1.03(8)
11.0	1.83(6)	6.83(6)	5.53(7)
14.0	8.07(5)	3.02(6)	2.66(7)
18.0	4.56(5)	1.93(6)	1.84(7)
23.0	3.27(5)	1.81(6)	2.42(7)
29.0	2.44(5)	1.21(6)	1.13(7)
36.0	1.62(5)	8.09(5)	5.97(6)
45.0	1.77(5)	8.13(5)	4.22(6)
57.0	1.23(5)	4.17(5)	1.65(6)
72.0	6.61(4)	1.26(5)	2.73(5)
90.0	4.90(4)	8.46(4)	1.58(5)
110.0	3.17(4)	4.32(4)	6.12(4)
140.0	2.02(4)	2.63(4)	3.54(4)
180.0	1.42(4)	1.74(4)	2.23(4)
230.0	5.64(3)	6.71(3)	8.50(3)
290.0	1.13(3)	1.30(3)	1.61(3)
360.0	1.18(2)	1.38(2)	1.75(2)

†Decadic exponents are enclosed in parentheses.

Table 5. Electron Production and Loss Rates

Process	Rate (electrons cm^{-3} sec^{-1}) 180 km	200 km	250 km
Photoionization (PI)			
$O(^3P)$	7.6	29.4	117.9
$N_2(X\ ^1\Sigma_g^+)$	4.0	11.8	38.5
$O_2(X\ ^3\Sigma_g^-)$	8.3	6.4	4.4
$NO(X\ ^2\Pi)$	6.8	3.6	1.3
Total	26.7	51.2	162.1
Collisional Ionization (CI)			
$O(^3P)$	15.1	30.5	68.2
$N_2(X\ ^1\Sigma_g^+)$	13.0	17.2	15.9
$O_2(X\ ^3\Sigma_g^-)$	1.2	1.4	1.0
Total	29.3	49.1	85.1
Dissociative Recombination (DR)			
$NO^+(X\ ^1\Sigma^+)$	661.1	715.4	894.6
$O_2^+(X\ ^2\Pi_g)$	203.7	298.7	224.2
$N_2^+(X\ ^2\Sigma_g^+)$		0.9	68.7
Total	864.8	1015.0	1187.5
DR/(PI + CI)	15.4	10.1	4.8

Table 6. Relative Rates of Formation of Species from Photoabsorption and Slowing-Down Photoelectrons

Species	Relative Rates of Formation			Species	Relative Rates of Formation		
	180 km	200 km	250 km		180 km	200 km	250 km
$O(^3P)$	0.14	0.05	-	$N(^4S°)$	0.01	-	-
$O(^1D)$	0.26	0.23	0.16	$N_2(X\ ^1\Sigma_g^+)v'$	0.18	0.20	0.08
$O(^1S)$	0.01	0.01	0.01	$N_2(A\ ^3\Sigma^+)$	0.11	0.11	0.06
$O(3s\ ^3S°)$	0.01	0.02	0.03	$N_2(B\ ^3\Pi_g)$	0.02	0.02	0.02
$O(3s\ ^3P)$	0.02	0.045	0.10	$N_2(a\ ^1\Pi_g)$	0.01	0.01	0 01
$O^+(^4S°)$	0.04	0.08	0.18	$N_2(c\ ^3\Pi_u)$	0.01	0.015	0.01
$O^+(^2D°)$	0.03	0.05	0.11	$N_2^+(X\ ^2\Sigma_g^+)$	0.015	0.02	0.035
$O^+(^2P°)$	0.015	0.025	0.06	$N_2^+(A\ ^2\Pi_u)$	0.03	0.04	0.05
$O_2^+(X\ ^2\Pi_g)$	0.03	0.02	-	$N_2^+(B\ ^2\Sigma_u^+)$	0.01	0.01	0.01
$O_2^+(a\ ^4\Pi_u)$	0.01	-	-				

Table 7. Relative Rates of Change in Energy Modes after Photoabsorption and after Establishment of Electron Energy Distribution

$\dot{M}$*	180 km		200 km		250 km	
	PA†	SS†	PA	SS	PA	SS
$\dot{E}$	0.45	0.04	0.53	0.05	0.52	0.12
$\dot{K}$	0.06	0.07	0.02	0.03	~0.0	~0.0
$\dot{R}$	0.10	0.19	0.10	0.23	0.06	0.21
$\dot{X}_v$	~0.0	0.01	0.0	0.01	~0.0	~0.0
$\dot{D}$	0.10	0.11	0.03	0.04	0.01	0.01
$\dot{I}$	0.16	0.36	0.22	0.43	0.34	0.52
$\dot{X}_e$	0.13	0.22	0.10	0.21	0.07	0.14

*$\dot{M} \equiv dM/dt$; E, electron translation; K, heavy-particle translation; R, radiation; X_v, vibrational excitation; D, dissociation; I, ionization; X_e, electronic excitation. Reference state is $N_2(X\ ^1\Sigma_g^+) + O_2(X\ ^3\Sigma_g^-)$.

†PA ≡ photoabsorption; SS ≡ steady state in high-energy electron subset.

Figure Captions

1 Differential electron-energy spectra for electron collisional ionization of $N_2(X\ ^1\Sigma_g^+)$: Comparison of model in this paper (X = 0 in equation 13) with experimental data of Opal et al. (1971).

2 Electron-flux spectra for a sample problem in which the photoelectrons lose their energy by only Coulomb collisions with ambient electrons: Comparison of simple model with rigorous treatment of Krinberg (1973). See Section 2.2 for detailed conditions.

3 Calculated and measured electron-flux spectra at White Sands, N. M. on February 8, 1971, for altitudes (and solar zenith angles) of 180 km ($\chi \approx 90.2°$), approximately 200 km ($\chi \approx 90.1°$), and 250 km ($\chi \approx 90.0°$). Smooth curves represent measurements (Hays and Sharp, 1973); histogram-like curves represent results of calculations. Note the broken abscissa.

4 Calculated electron-flux values in the energy range from 14 to 36 eV at altitudes of 200 and 250 km: Comparison of electron-flux values with (X) and without (O) the contributions from electrons formed by absorption of the He II 303.8 Å solar line by $O(^3P)$ and $N_2(X^1\Sigma_g^+)$. The values of the fluxes are plotted at the characteristic energies of the energy groups (see Table 1).

5 Calculated electron-flux values in the energy range from 29 to 90 eV at altitudes of 180, 200, and 250 km: Comparison of electron-flux values with (X) and without (O) the contributions from electrons formed by photoabsorption of radiation in the wavelength interval from 153 to 205 Å. The values of the fluxes are plotted at the characteristic energies of the energy groups (see Table 1).

6 Calculated differential production rate for photoelectrons in the energy range from 20 to 30 eV at 200 km for $\chi \cong 90.^{\circ}1$. The ion products and the associated electron energies (eV) for the peak values are: $O^+(^4S^\circ)$ - 20.05, 23.33, 27.18, 30.01; $O^+(^2D^\circ)$ - 20.02, 23.87, 26.7; $O^+(^2P^\circ)$ - 22.18, 25.01; $N_2^+(X\ ^2\Sigma_g^+)$ - 21.37, 25.22, 28.05; $N_2^+(A\ ^2\Pi_u)$ - 20.37, 24.22, 27.05; $N_2^+(B\ ^2\Sigma_u^+)$ - 22.05, 24.88.

Figure 1

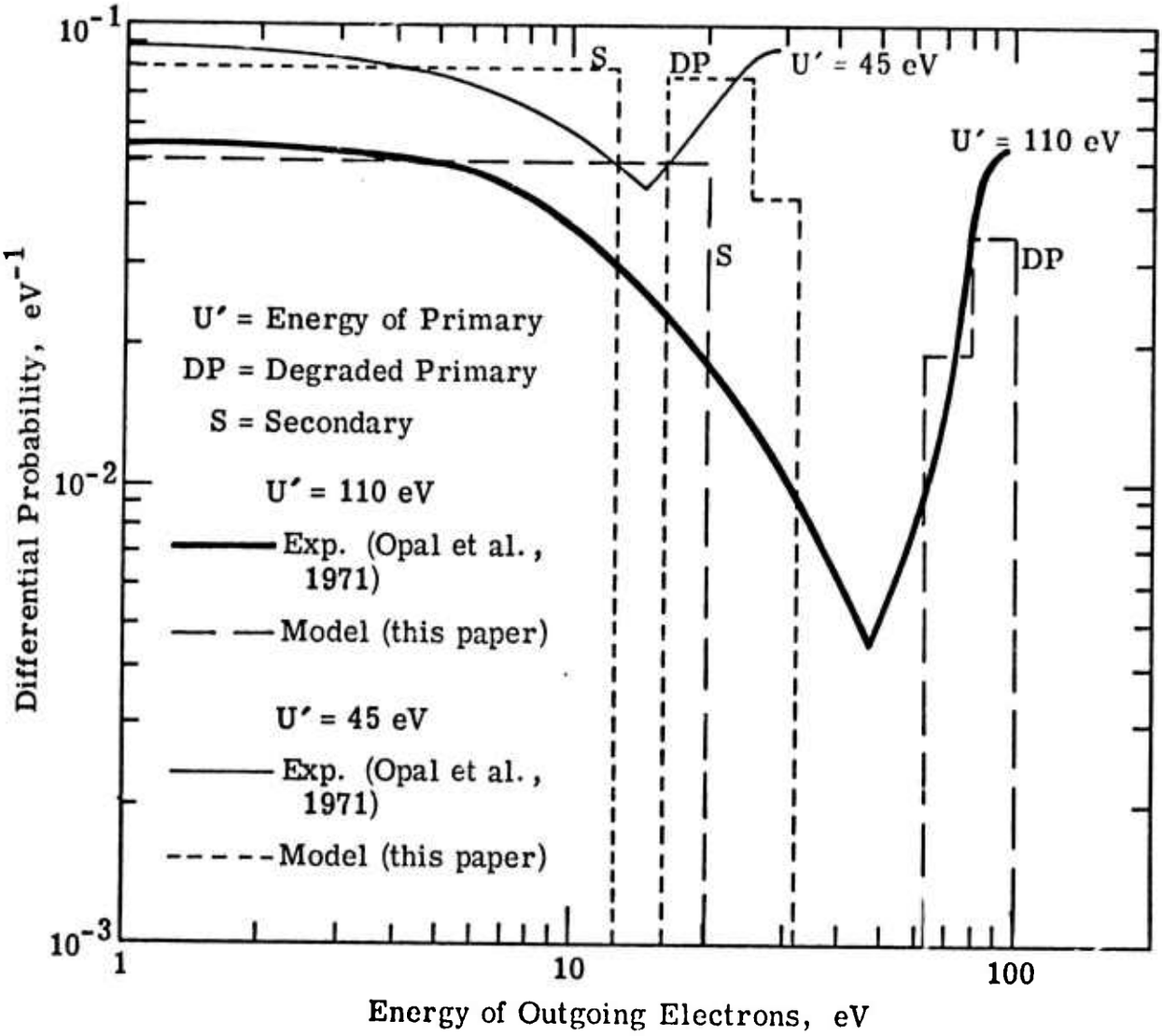
10^{-1}
10^{-2}
10^{-3}
Differential Probability, eV^{-1}
S
DP
U′ = 45 eV
U′ = 110 eV
S
DP
U′ = Energy of Primary
DP = Degraded Primary
S = Secondary
U′ = 110 eV
Exp. (Opal et al., 1971)
Model (this paper)
U′ = 45 eV
Exp. (Opal et al., 1971)
Model (this paper)
1
10
100
Energy of Outgoing Electrons, eV

Figure 2

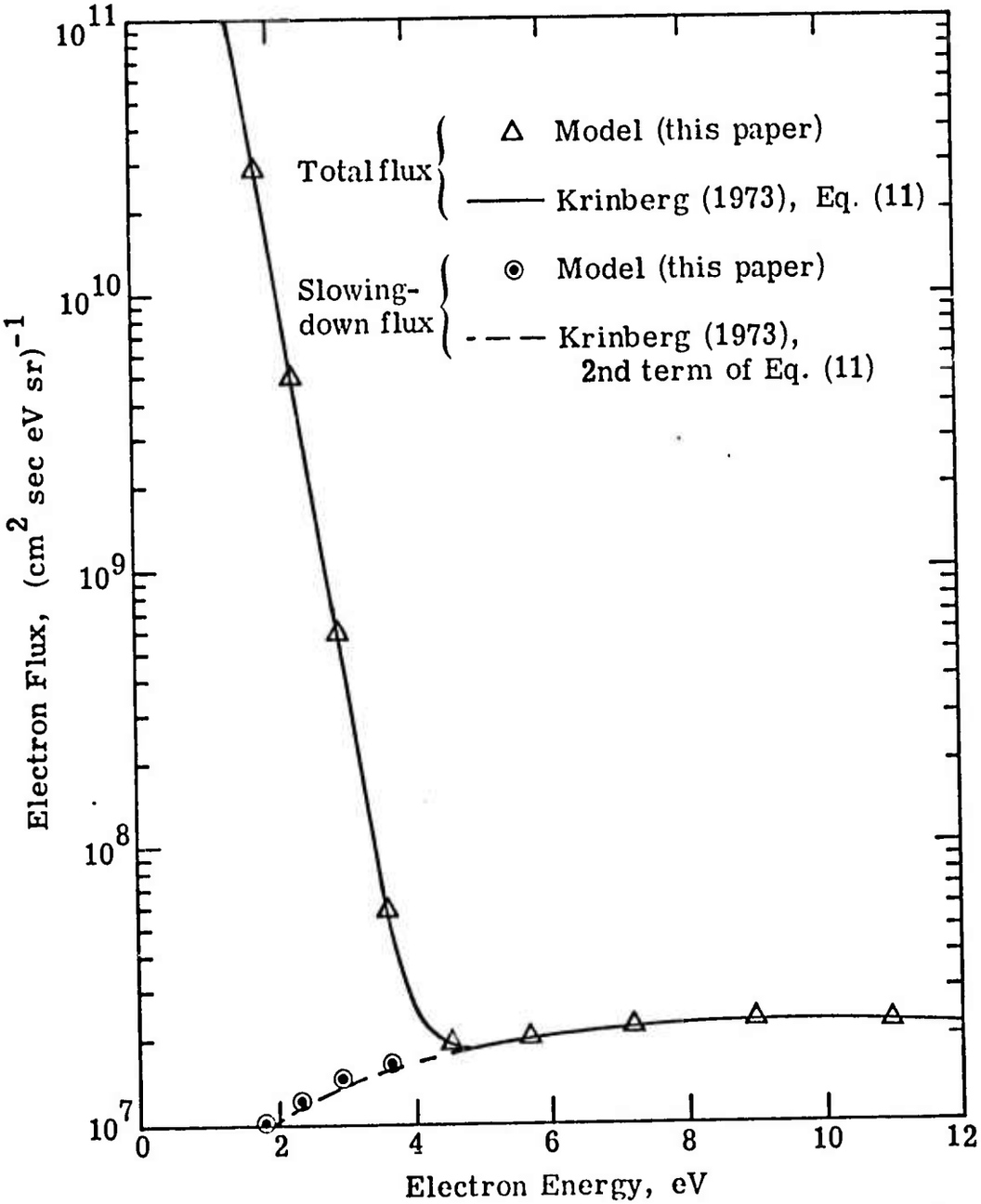
Total flux
Model (this paper)
Krinberg (1973), Eq. (11)
Slowing-down flux
Model (this paper)
Krinberg (1973), 2nd term of Eq. (11)
Electron Flux, (cm^2 sec eV sr)$^{-1}$
Electron Energy, eV
10^{11}
10^{10}
10^9
10^8
10^7
0
2
4
6
8
10
12

Figure 3

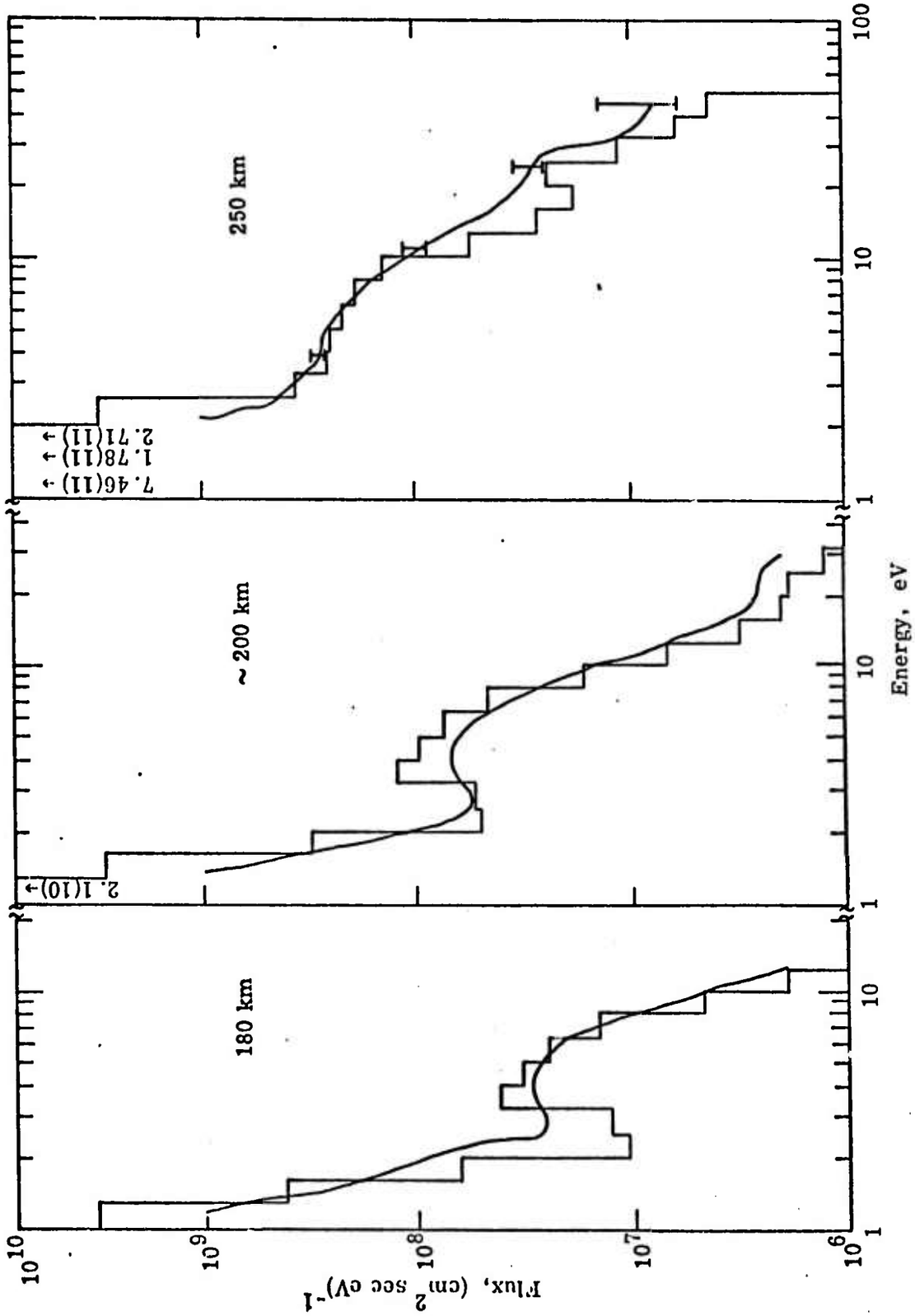
250 km
7.46(11)→
1.78(11)→
2.71(11)→
~ 200 km
2.1(10)→
180 km
Flux, (cm)^2 sec eV)$^{-1}$
Energy, eV
10^{10}
10^9
10^8
10^7
10^6
1
10
100

Figure 4

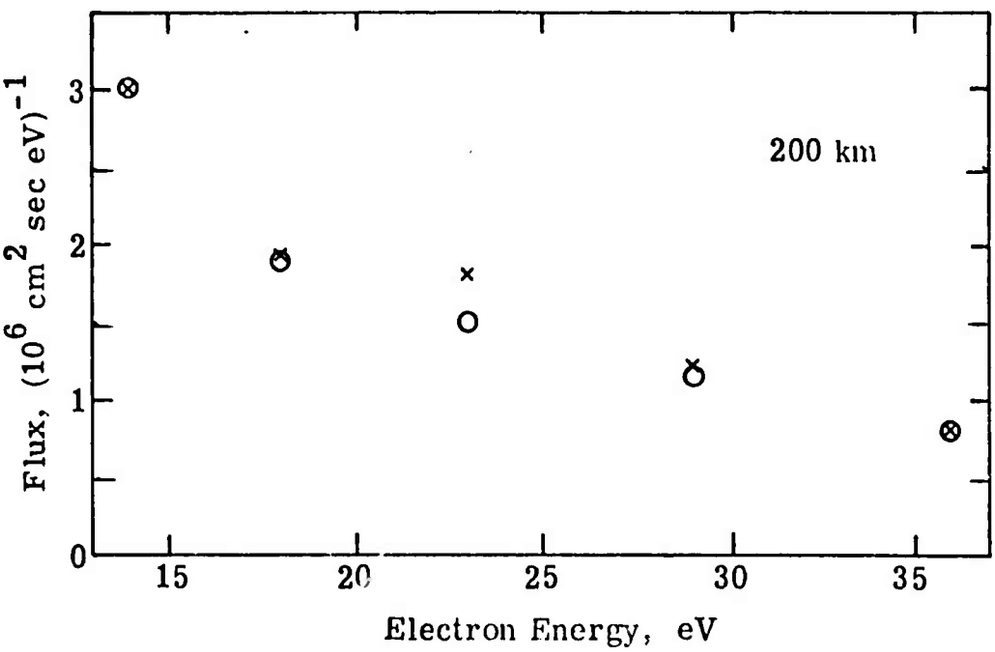
200 km
Flux, $(10^6$ cm^2 sec eV$)^{-1}$
0
1
2
3
15
20
25
30
35
Electron Energy, eV

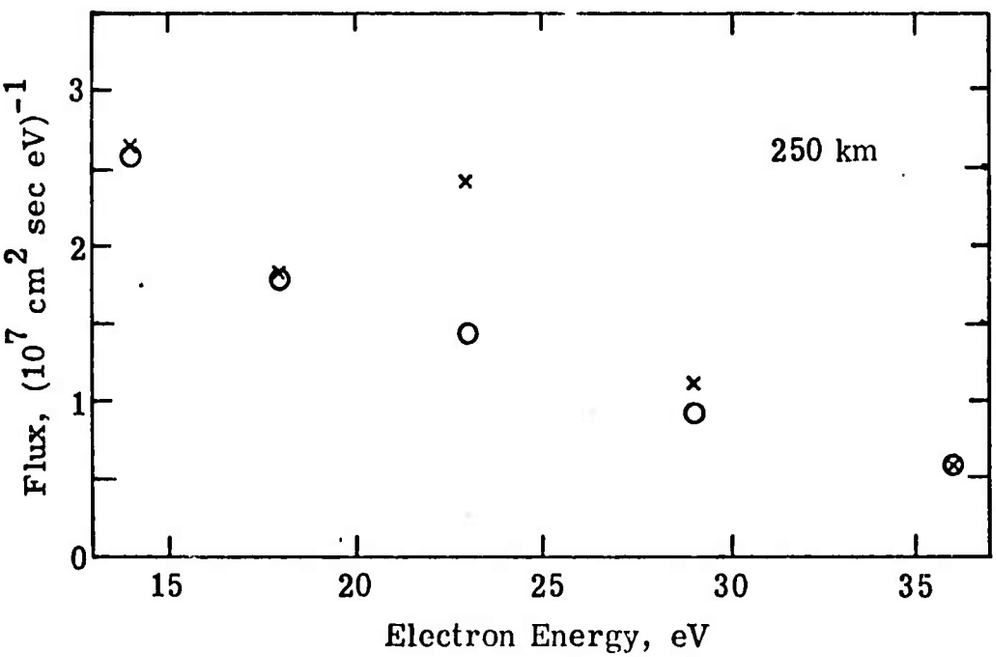
250 km
Flux, $(10^7$ cm^2 sec eV$)^{-1}$
0
1
2
3
15
20
25
30
35
Electron Energy, eV

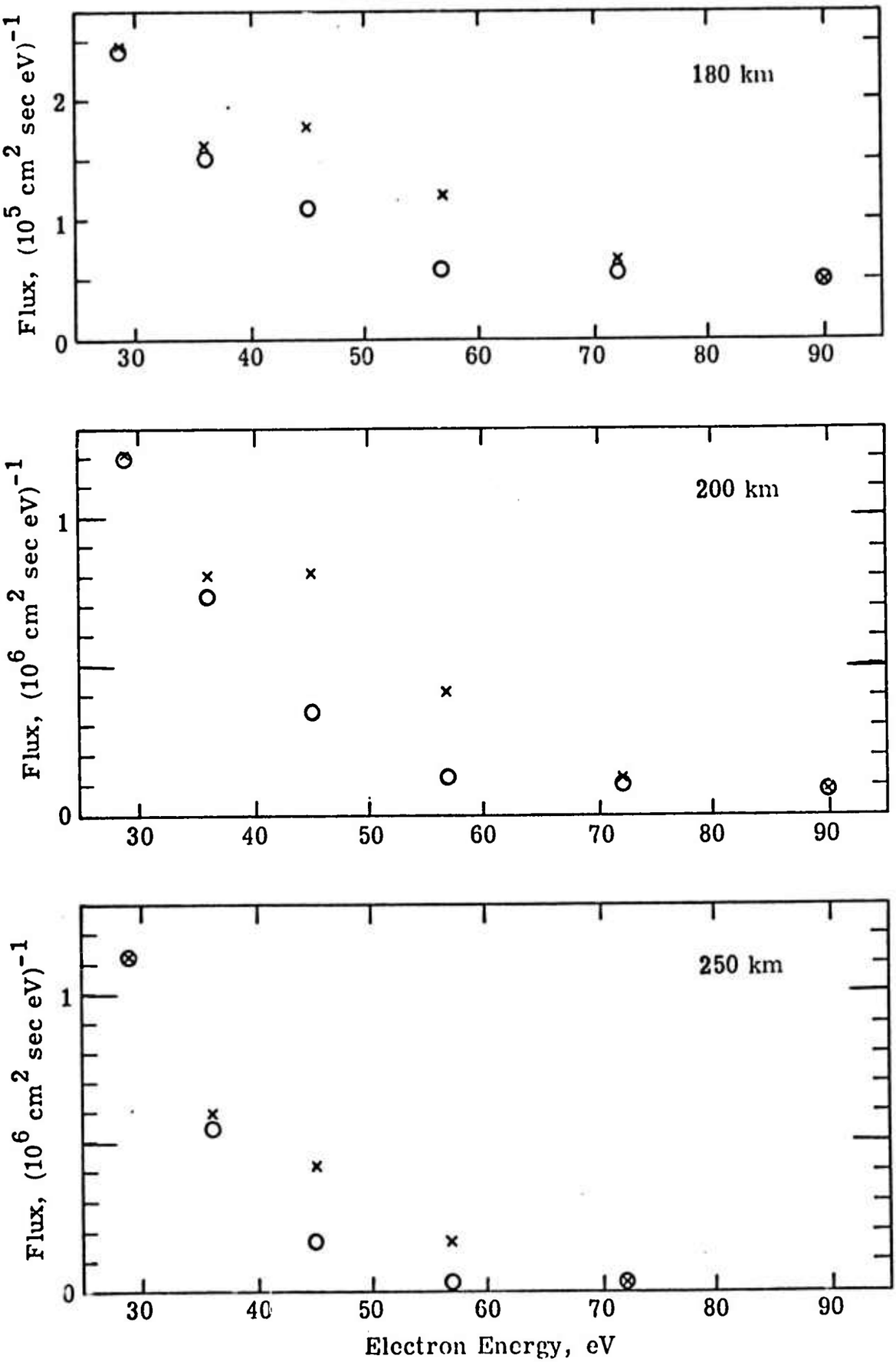
180 km
200 km
250 km
Flux, $(10^5$ cm^2 sec eV$)^{-1}$
Flux, $(10^6$ cm^2 sec eV$)^{-1}$
Flux, $(10^6$ cm^2 sec eV$)^{-1}$
Electron Energy, eV

Figure 6

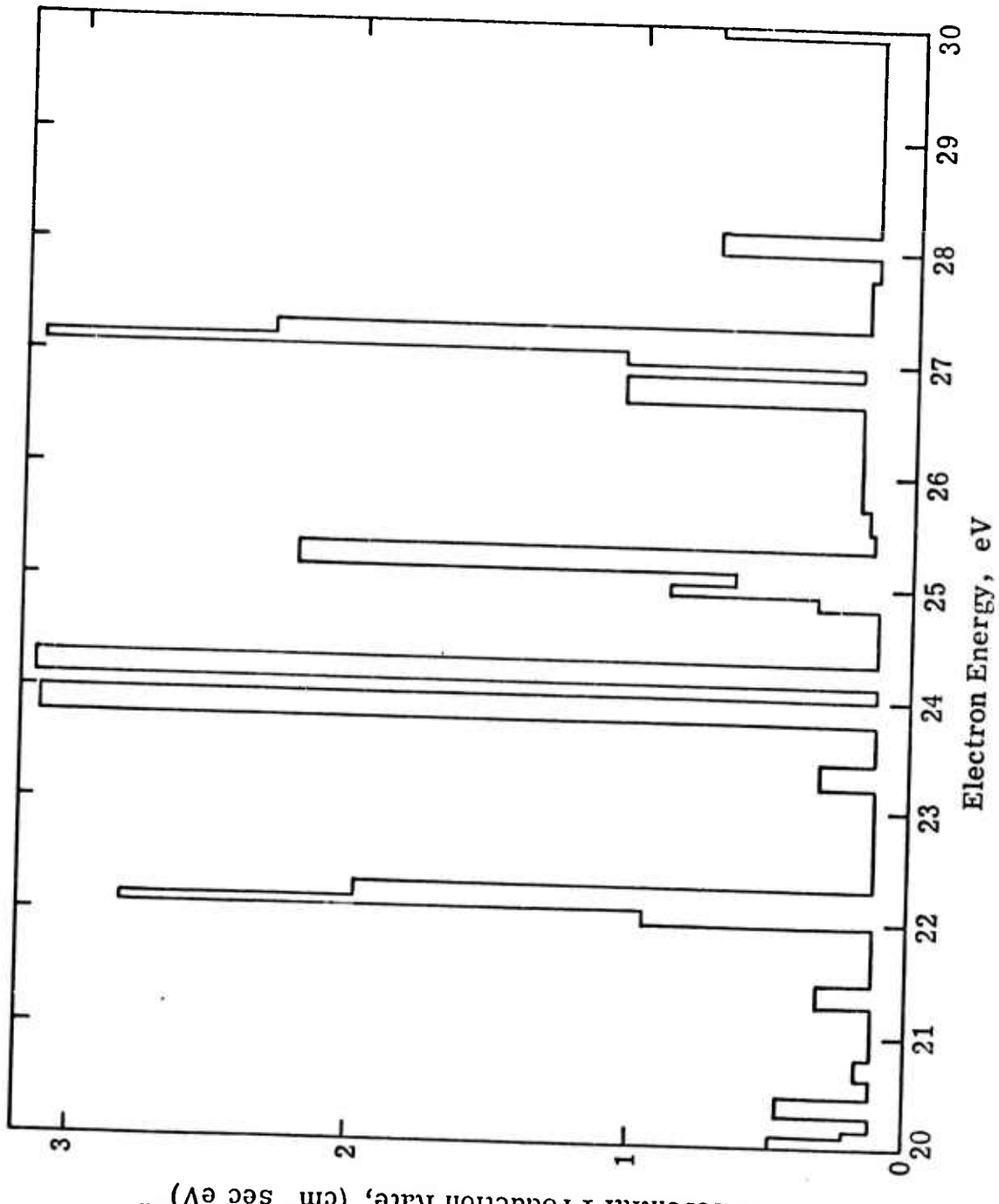
Differential Production Rate, (cm^3 sec eV)$^{-1}$
0
1
2
3
20
21
22
23
24
25
26
27
28
29
30
Electron Energy, eV

SECTION 3

THE EFFECT OF UNCERTAINTIES IN RATE COEFFICIENTS ON DENSITIES OF E-REGION SPECIES

The Effect of Uncertainties in Rate Coefficients on Densities of E-Region Species

B. F. Myers, D. A. Hamlin,
M. R. Schoonover, and J. I. Valerio
Science Applications, Inc., La Jolla, California 92037

A direct statistical method has been applied to determine the effect of uncertainties in rate coefficients on computed densities of E-region species. Uncertainties in rate coefficients are described in terms of Gaussian error-law distributions with a common fractional standard deviation. Mean densities are found to be relatively insensitive to rate-coefficient uncertainties; fractional standard deviations of density distributions are, in general, less than twice those associated with rate-coefficient distributions, provided the latter fractional standard deviations are not greater than 0.45.

Many reactions are necessary to describe chemical processes in the atmosphere. In such chemical systems, it is difficult to evaluate inaccuracies in the computed species densities. These inaccuracies stem from uncertainties in the input data and from omissions or approximations of relevant physical and chemical processes. One of the uncertainties, that associated with reaction-rate coefficients, is treated here by a direct statistical method for the case of an E region chemical reaction system

operating over short time intervals. The calculations presented here are meant to be illustrative rather than exhaustive.

Sufficient information about the errors and the distribution of errors associated with measurements of rate coefficients is not generally available. Accordingly, in the calculations described here, uncertainties in the rate coefficients were assumed to be describable in terms of the Gaussian error-law with a mean value of the rate coefficient, k_o, and a standard deviation, s; the effects of variations in s on species densities and their distributions were examined. For simplicity, a common fractional standard deviation was assigned to the rate-coefficient distributions.

Consider a system consisting of n reactions and corresponding rate coefficients; let $m(\leq n)$ of the rate coefficients have uncertainties describable in terms of the Gaussian error-law distribution. A set of rate coefficients, $\{k_j\}$, is formed by randomly selecting from each k_j-distribution for j equals 1 to m. The set of m rate coefficients and the remaining n-m coefficients are used to calculate the species densities by integrating the differential equations describing the system over some interval of time. The selection of the set $\{k_j\}$ and the integration of the differential equations are repeated a number of times to obtain an indication of the true mean value and spread in species densities.

The random values of k_j were sampled from the assumed distribution by use of the rejection technique [Kahn, 1956]. Random numbers used in this technique were generated by an adaptation [McGrath and Irving, 1973]

of the standard, multiplicative congruential method [Coveyou and MacPherson, 1967]; the adaptation is independent of the computer used to generate the numbers. With the use of the Gaussian error-law distribution, values of $k_j < 0$ occur in the sampling process; the number of such values increases as s increases. These values of k_j were discarded. The number discarded for the calculations described here exceeds 0.05% of the total sample population only for the largest value of s used; in this case, 1.5% of the sampled k_j was discarded. In practice, the retained values of k_j were equal to or greater than $10^{-2}\ k_o$ (and, also by choice, equal to or less than $10^2\ k_o$).

The set of reactions representing the E-region system is given in Table 1; the system was used under conditions applying to an altitude of approximately 140 km. For this system, n = 25 and m = 17; the relative values of rate coefficients for reactions 1 through 8 and for reactions 10 and 11 were kept constant while the absolute values of the rate coefficients for reactions 1 and 10 were varied in the manner described above. The differential equations for the species densities were integrated over a problem-time interval of six minutes for each of 3000 sets $\{k_j\}$. By six minutes in problem time, initial transients were unimportant. For 3000 runs of six minutes in problem time, 2-1/3 minutes of CP time on a CDC 7600 computer were required. An additional calculation with the set of rate coefficients listed in Table 1 was also made. The initial species densities are listed in Table 2 for the starting time of the

calculation, 1200 hrs. For each set of 3000 calculations, the error-law distribution of rate-coefficient values was characterized by the mean value of the rate coefficient, k_o, referred to below as the nominal value, and by a fractional standard deviation, $f_{sk} \equiv s/k_o$, of 0.15, 0.30, and 0.45 in successive sets of calculations.

The results of the calculations are summarized in Table 3. Consider first the group of species consisting of the charged particles plus $N(^2D^\circ)$. The following features are noted for this group: (1) The average species densities depart by less than 10% from the species densities calculated by using the set of nominal rate coefficients, provided $f_{sk} \leq 0.30$. (2) The fractional standard deviations for species densities, f_{sn}, are, roughly, between one and two times f_{sk}. Furthermore, f_{sn} increases monotonically with decrease in density, n, except for N_2^+. The increase in f_{sn} is roughly a factor of two for a decrease in n from about 10^5 cm^{-3} to about 10^1 cm^{-3}. (3) The density distributions have pronounced positive coefficients-of-skewness, β, which increase with increasing f_{sk}.

The source of the positive skewness can be appreciated with a simple example. Consider the species densities to be in a steady-state condition, a reasonable assumption for the present calculations. Let the nominal rate coefficients associated with production processes for a given species be multiplied by the factor $(1 + \epsilon)$ while those associated with the loss processes of the given species be multiplied by the factor $(1 - \epsilon)$. Then the nominal value of the density of the given species, n_o, will be

multiplied by the factor $F \equiv (1 + \epsilon)/(1 - \epsilon)$. In the inverse case, the nominal value of the density will be multiplied by F^{-1}. On a linear scale of density, $n_o F^{-1}$ will be closer to n_o than $n_o F$ is to n_o; hence, the positive skewness obtains.

The increases in f_{sn} and β with increasing f_{sk}, as shown in Table 3 for the group consisting of charged particles plus $N(^2D^\circ)$, is illustrated in Fig. 1 where a typical set of histograms is drawn; the species represented is NO^+. The class intervals in these differential frequency histograms are equal to 0.2 of the standard deviation of the density distribution for each of the three f_{sk} cases. (Note that the means, standard deviations, and coefficients of skewness in Table 3 were calculated from the original set of 3000 densities prior to constructing the histograms.) The mean density value for each distribution is indicated by the placement of the associated arrow. One sees that, as f_{sk} increases, the mean density and the spread of the distribution increase. Also, the large values of β evidently arise from a small number of calculations yielding high densities. For the group of species consisting of charge particles plus $N(^2D^\circ)$, such calculations which yield densities beyond 2.5 standard deviations from the mean density represent less than 3% of the total number of calculations for $f_{sk} = 0.45$; for the smaller values of f_{sk}, such percentages are much smaller. When calculations of the standard deviation and coefficient of skewness were made with densities lying within 2.5 standard deviations of

the previously computed means, then for $f_{sk} = 0.30$, the values of s were reduced by only 12 to 24% whereas values of β were decreased by 65 to 90%.

For the group consisting of the last five species in Table 3, the following features occur: (1) The average densities are the same as those calculated by using the set of nominal rate coefficients. (2) The fractional standard deviations for species densities are small but increase with increasing f_{sk}. (3) The skewness of the density distributions is small.

The above calculations were repeated, for $f_{sk} = 0.30$, by using a different sequence of random numbers from the random number generator. Use of the new sequence did not result in any essential changes. To obtain an indication of the effect of restricting the k_j to values equal to or greater than $10^{-2}\, k_o$, the above calculations were repeated by using the subset of reactions 4, 19, and 20 which is not coupled to the reaction system (assuming constant densities for O, O_2, and N_2) but yet describes completely the processes involving one of the species, $O^+(^2D^\circ)$. The changes occurring with limits of k_j given by $k_o(1 \pm 0.99)$, rather than $k_o(1 + 99)$ and $k_o(1 - 0.99)$ as above, were not larger than in the cases of using different sequences of random numbers.

For simplicity in these calculations, the problem of assessing the errors given to experimental values of rate coefficients has been circumvented. If one consults a listing of such errors for the chemical reactions of Table 1, as for example, Bortner and Baurer [1973], and assumes that the errors given represent one standard deviation in a Gaussian distribution

of rate-coefficient values, then, for the current state of knowledge about the accuracy of rate coefficients, the best representative for a calculation of the above type would be one using $0.30 \leq f_{sk} < 0.45$. Note that if the assumption were acceptable, a more reliable calculation could be made with the present method since different f_{sk} can readily be assigned to different rate coefficients.

The direct statistical method used above has the disadvantage that for long problem-times, the method is expensive. Yet, the distributions of species densities will change with time so that the time dependence can be important. The above application is also limited by use of the Gaussian error-law distribution which will become a poorer representation as the standard deviation in the rate-coefficient distribution increases; this limitation can be readily overcome by using a more appropriate distribution function. Finally, the above method does not readily give information about the relative importance of rate coefficients. For the interested reader, reference is given to the related work of Cukier et al. [1973] and Schaibly and Shuler [1973] in which a method is given for identifying those rate coefficients which significantly affect species densities.

Acknowledgements. This research was supported by the Defense Advanced Research Projects Agency of the Department of Defense and was monitored by the Office of Naval Research under Contract No. N00014-72-C-0292.

REFERENCES

Black, G., T. G. Slanger, G. A. St. John, and R. A. Young, Vacuum-ultraviolet photolysis of N_2O, IV. Deactivation of $N(^2D)$, J. Chem. Phys., 51, 116-121, 1969.

Bortner, M. H., and T. Baurer (Eds.), DNA Reaction Rate Handbook, Tech. Rep. DNA 1948H, 2d ed., rev. 2 (in press), Ch. 24, Defense Nuclear Agency, Washington, D. C., 1973.

Breig, E. L., M. E. Brennan, and R. J. McNeal, Effect of atomic oxygen on the N_2 vibrational temperature in the lower thermosphere, J. Geophys. Res., 78, 1225-1228, 1973.

Clark, I. D., and R. P. Wayne, Kinetics of the reaction between atomic nitrogen and molecular oxygen in the ground ($^3\Sigma_g^-$) and first excited ($^1\Delta_g$) state, Proc. Roy. Soc. Lond., A316, 539-550, 1970.

COSPAR International Reference Atmosphere (CIRA) 1965, North-Holland, Amsterdam, Holland, 1965.

Coveyou, R. R., and R. D. MacPherson, Fourier analysis of uniform random number generators, J. Assoc. Comp. Mach., 14, 100-119, 1967.

Cukier, R. I., C. M. Fortuin, K. E. Shuler, A. G. Petschek, and J. H. Schaibly, Study of the sensitivity of coupled reaction systems to uncertainties in rate coefficients, I. Theory, J. Chem. Phys., 59, 3873-3878, 1973.

Cunningham, A. J., and R. M. Hobson, Dissociative recombination at elevated temperatures, III. O_2^+ dominated afterglows, J. Phys., B5, 2320-2327, 1972.

Dunkin, D. B., F. C. Fehsenfeld, A. L. Schmeltekopf, and E. E. Ferguson, Ion-molecule reactions studies from 300° to 600°K in a temperature-controlled flowing afterglow system, J. Chem. Phys., 49, 1365-1371, 1968.

Fehsenfeld, F. C., D. B. Dunkin, and E. E. Ferguson, Rate constants for the reaction of CO_2^+ with O, O_2, and NO; N_2^+ with O and NO; and O_2^+ with NO, Planet. Space Sci., 18, 1267-1269, 1970.

Goldan, P. D., A. L. Schmeltekopf, F. C. Fehsenfeld, H. I. Schiff, and E. E. Ferguson, Thermal energy ion-neutral reaction rates, II. Some reactions of ionospheric interest, J. Chem. Phys., 44, 4095-4103, 1966.

Hinteregger, H. E., The extreme ultraviolet solar spectrum and the variation during a solar cycle, Ann. Geophys., 26, 547-554, 1970.

Johnsen, R., and M. A. Biondi. Measurements of the $O^+ + N_2$ and $O^+ + O_2$ reaction rates from 300°K to 2 eV, J. Chem. Phys., 59, 3504-3509, 1973.

Johnsen, R., H. L. Brown, and M. A. Biondi, Ion-molecule reactions involving N_2^+, N^+, O_2^+, and O^+ ions from 300°K to ~ 1 eV, J. Chem. Phys., 52, 5080-5084, 1970.

Kahn, H., Applications of Monte Carlo, Tech. Rep. AECU-3259, p. 39, United States Atomic Energy Commission, Technical Information Service Extension, Oak Ridge, Tenn., Rev. 27 April 1956.

Lin, C., and F. Kaufman, Reactions of metastable nitrogen atoms, J. Chem. Phys., 55, 3760-3770, 1971.

McGrath, E. J., and D. C. Irving, Techniques for efficient Monte Carlo simulation, Vol. II: Random number generation for selected probability distributions, Tech. Rep. SAI-72-590-LJ, p. 99, Science Applications, Inc., La Jolla, Calif., March 1973.

Mehr, F. J., and M. A. Biondi, Electron temperature dependence of recombination of O_2^+ and N_2^+ ions with electrons, Phys. Rev., 181, 264-271, 1969.

Michels, H. H., Dissociative recombination of $e + N_2^+$, paper presented at the Third International Conference on Atomic Physics, Internat. Un. Pure Appl. Phys., Boulder, Colo., August 7-11, 1972.

Neynaber, R. H., J. A. Rutherford, and D. A. Vroom, A study of ion-neutral reactions of importance in the upper atmosphere, Tech. Rep. DNA 3134F, pp. 19-20, Intelcom Rad Tech, San Diego, Calif., July 1973.

Rutherford, J. A., and D. A. Vroom, Effect of metastable $O^+(^2D)$ on reactions of O^+ with nitrogen molecules, J. Chem. Phys., 55, 5622-5624, 1971.

Schaibly, J. H., and K. E. Shuler, Study of the sensitivity of coupled reaction systems to uncertainties in rate coefficients, II. Applications, J. Chem. Phys., 59, 3879-3888, 1973.

Schiff, H. I., Neutral reactions involving oxygen and nitrogen, Can. J. Chem., 47, 1903-1916, 1969.

Slanger, T. G., B. J. Wood, and G. Black, Temperature coefficients for $N(^2D)$ quenching by O_2 and N_2O, J. Geophys. Res., 76, 8430-8433, 1971.

Strobel, D. F., Minor neutral constituents in the mesosphere and lower thermosphere, Radio Sci., 7, 1-21, 1972.

Van Zandt, T. E., and T. F. O'Malley, Rate coefficient for the reaction of O^+ with vibrationally excited N_2, J. Geophys. Res., 78, 6818-6820, 1973.

Walls, F. L., and G. H. Dunn, Electron-positive ion recombination studies using ion storage techniques (abstract), Bull. Am. Phys. Soc., 19, 150-151, 1974.

Weller, C. S., and M. A. Biondi, Recombination, attachment, and ambipolar diffusion of electrons in photo-ionized NO afterglows, Phys. Rev., 172, 198-206, 1968.

Table 1

Processes and Nominal Values for Rate Coefficients

Reaction No.	Process[a]	k_0 for 1200 hr[b]	Reference
1	$N_2 + h\nu \rightarrow N_2^+ + e$	3.0(-8)	c
2	$O_2 + h\nu \rightarrow O_2^+ + e$	7.0(-8)	c
3	$O + h\nu \rightarrow O^+ + e$	1.2(-8)	c
4	$O + h\nu \rightarrow O^+(^2D^\circ) + e$	1.3(-8)	c
5	$NO + h\nu \rightarrow NO^+ + e$	7.8(-7)	c
6	$N_2 + h\nu \rightarrow 2N$	4.6(-10)	c
7	$O_2 + h\nu \rightarrow 2O$	1.7(-7)	c
8	$NO + h\nu \rightarrow N + O$	2.3(-7)	c
9	$O_2^+ + e \rightarrow O + O$	1.2(-7)	d, e
10	$NO^+ + e \rightarrow N + O$	4.4(-8)	f, g
11	$NO^+ + e \rightarrow N(^2D^\circ) + O$	1.8(-7)	f, g
12	$N_2^+ + e \rightarrow N(^2D^\circ) + N$	1.3(-7)	e, h
13	$N_2^+ + O_2 \rightarrow N_2 + O_2^+$	3.0(-11)	i, j
14	$N_2^+ + O \rightarrow NO^+ + N$	1.4(-10)	k, l
15	$O^+ + O_2 \rightarrow O + O_2^+$	1.5(-11)	i, m
16	$O^+ + N_2 \rightarrow NO^+ + N$	6.3(-13)	i, m, n, o
17	$O_2^+ + NO \rightarrow O_2 + NO^+$	6.3(-10)	j, k
18	$O_2^+ + N \rightarrow NO^+ + O$	1.8(-10)	p
19	$O^+(^2D^\circ) + O_2 \rightarrow O + O_2^+$	3.6(-10)	q
20	$O^+(^2D^\circ) + N_2 \rightarrow O + N_2^+$	4.5(-10)	r

Table 1 (Continued)

Reaction No.	Process[a]	k_o for 1200 hr[b]	Reference
21	$N + O_2 \rightarrow NO + O$	4.3(-14)	s
22	$N(^2D^\circ) + O_2 \rightarrow NO + O$	9.9(-12)	t, u
23	$N(^2D^\circ) + O \rightarrow N + O$	1.0(-12)	no data; estimated
24	$N + NO \rightarrow N_2 + O$	2.2(-11)	v
25	$N(^2D^\circ) + NO \rightarrow N_2 + O$	1.3(-10)	t, w

[a] Only ground electronic states are involved unless indicated otherwise.

[b] The neutral particle temperature was taken from the CIRA-65 Model-5 atmosphere to be 610°K for 1200 hrs; units of k_o are sec^{-1} for processes 1 to 8 and $cm^3\ sec^{-1}$ for the remaining processes. The decadic exponent is enclosed by parentheses.

[c] Calculated with solar flux routine using flux values and photon group structure recommended by Hinteregger [1970], for conditions of 1200 hrs at 140 km with solar zenith angle of 21.6°.

[d] Cunningham and Hobson [1972].

[e] Mehr and Biondi [1969].

[f] Weller and Biondi [1968].

[g] Walls and Dunn [1973].

[h] Michels [1972].

[i] Dunkin et al. [1968].

[j] Johnsen et al. [1970].

[k] Fehsenfeld et al. [1970].

[l] Neynaber et al. [1973].

[m] Johnsen and Biondi [1973].

[n] Breig et al. [1973].

[o] Van Zandt and O'Malley [1973].

[p] Goldan et al. [1966].

[q] J. A. Rutherford (unpublished data, 1973).

[r]Rutherford and Vroom [1971].

[s]Clark and Wayne [1970].

[t]Lin and Kaufman [1971].

[u]Slanger et al. [1971].

[v]Schiff [1969].

[w]Black et al. [1969].

Table 2

Initial Densities of Species at t_o = 1200 hrs*

Species	Density, cm^{-3}	Species	Density, cm^{-3}
N_2	6.4(10)	N_2^+	6.7(2)
O_2	9.7(9)	O_2^+	2.6(4)
O	2.2(10)	O^+	1.2(3)
NO^+	5.0(7)	$O^+(^2D^\circ)$	8.0(0)
N	1.9(6)	NO^+	8.1(4)
$N(^2D)$	3.3(4)	$e^‡$	≈1.1(5)

*t_o = starting time of calculation.

†Densities from Strobel [1972].

‡In the calculations, the electron density was set equal to the exact sum of ion densities.

Table 3

Summary of Results on Propagation of Rate-Coefficient Uncertainties for E-Region Densities

Species	n_o	$f_{sk} = 0.15$			$f_{sk} = 0.30$			$f_{sk} = 0.45$		
		$n_o/\langle n\rangle$	f_{sn}	β	$n_o/\langle n\rangle$	f_{sn}	β	$n_o/\langle n\rangle$	f_{sn}	β
N_2^+	6.42(2)	0.98	0.21	0.53	0.91	0.53	4.29	0.78	1.07	8.00
O_2^+	2.35(4)	0.99	0.18	0.51	0.96	0.38	1.20	0.90	0.60	2.22
O^+	1.42(3)	0.98	0.19	0.47	0.94	0.45	1.88	0.86	0.73	3.41
$O^+(^2D^\circ)$	8.86(0)	0.98	0.21	0.74	0.91	0.54	3.22	0.81	0.83	3.89
NO^+	1.01(5)	1.0	0.11	0.51	0.98	0.27	2.53	0.94	0.54	4.46
e	1.27(5)	0.99	0.10	0.27	0.97	0.21	1.58	0.93	0.44	3.61
$N(^2D^\circ)$	1.82(4)	0.99	0.19	0.49	0.95	0.42	1.35	0.90	0.68	2.72
N_2	6.40(10)	1.0	2(-6)	-0.25	1.0	4(-6)	-0.28	1.0	6(-6)	-0.33
N	1.95(6)	1.0	0.08	0.23	1.0	0.16	0.20	1.0	0.23	0.33
O_2	9.70(9)	1.0	2(-5)	-0.09	1.0	4(-5)	-0.10	1.0	6(-5)	-0.29
O	2.20(10)	1.0	2(-5)	0.08	1.0	4(-5)	0.11	1.0	5(-5)	0.27
NO	4.98(7)	1.0	3(-3)	0.15	1.0	5(-3)	0.13	1.0	7(-3)	0.04

n_o density of species computed with nominal rate-coefficient set.

$\langle n\rangle$ average density of species computed with 3000 sets of randomly-selected rate coefficients.

f_{sx} $sx/\langle x\rangle$, where sx is the standard deviation of the x-distribution and x=k for rate-coefficient distribution and x=n for density distribution of species.

β skewness coefficient = third central moment/(standard deviation)^3

Fig. 1. Differential frequency histograms for NO^+ in cases of $f_{sk} = 0.15$, 0.30, and 0.45. The class intervals are equal to 0.2 times the standard deviation for each of these cases. Note the change of scales for the lower panel in which the histograms are extended above densities of 2×10^5 cm^{-3}. The mean density value for each distribution is indicated by the placement of the associated arrow.

Figure 1

Differential Frequency/(10^{-1}cm^{-3})
Density of NO^+/(10^5cm^{-3})
f_{sk}=0.15
f_{sk}=0.30
f_{sk}=0.45
1.0
0.5
0
2.0
1.5
1.0
0.5
0
0.02
0.01
0
2
3
4
5
6

SECTION 4

IONOSPHERIC-ELECTRON HEATING BY DISSOCIATIVE RECOMBINATION

Research Note

Ionospheric-Electron Heating by Dissociative Recombination

D. A. Hamlin and B. F. Myers
Science Applications, Inc., La Jolla, California 92037, U. S. A.

Abstract — It is shown that the loss of ionospheric electrons by dissociative recombination effectively heats the electron gas at a rate which is a few per cent of the main heating rate due to photoelectrons but which exceeds some of the rates for minor cooling processes frequently included in energy-balance studies.

A number of effects have been considered in the literature for heating and cooling the ionospheric electron gas (Stubbe and Varnum, 1972). In this Note we assess an overlooked effect of intermediate importance.

In the E and F regions, electrons are lost mainly by dissociative recombination with NO^+ and O_2^+. When an electron is lost, its kinetic energy, E, is removed from the thermal energy of the electron gas at temperature θ(eV). The electron gas is effectively heated if $E < 3\theta/2$ and cooled if $E > 3\theta/2$. The effective energy-return to the electron gas per recombination with a given molecular ion, ϵ, is

$$\epsilon = \frac{3}{2}\theta - \langle E \rangle \quad . \tag{1}$$

Here, for a dissociatively-recombining electron of velocity $v = \sqrt{2E/m}$ and cross-section $\sigma(E)$, its mean energy, $\langle E \rangle$, is given by

$$\langle E \rangle = k^{-1} \int_0^\infty E\, \sigma(E)\, v\, f(E)\, dE \quad , \tag{2}$$

where $f(E)$ is the Maxwellian energy-distribution function, and the rate coefficient corresponding to $\sigma(E)$ is

$$k \equiv \langle \sigma v \rangle = \int_0^\infty \sigma(E)\, v\, f(E)\, dE \quad . \tag{3}$$

The heating rate for the electron gas is

$$\dot{H} \equiv \frac{dH}{dt} = k\,[e]\,[i]\,\epsilon \quad , \qquad \text{eV cm}^{-3}\,\text{sec}^{-1} \tag{4}$$

where $[e]$ is the electron density and $[i]$ is the molecular-ion density.

The dependence of σ on E or of k on θ is not well established for ionospheric conditions. Thus, we shall consider a range of possibilities. For simplicity, we assume that the cross section can be expressed as a power law,

$$\sigma = \sigma_o\, E^{-n} \quad , \qquad n < 2 \quad . \tag{5}$$

Evaluation of Equations (2) and (3) with use of Equation (5) leads to the results

$$\frac{\langle E \rangle}{\theta} = \frac{\Gamma(3 - n)}{\Gamma(2 - n)} = 2 - n \quad , \qquad n < 2 \tag{6}$$

and

$$k = 2\sigma_o \sqrt{2/\pi m}\; \Gamma(2 - n)\, \theta^{-p} \quad , \tag{7}$$

where $\Gamma(x)$ is the gamma function and

$$p \equiv n - \frac{1}{2} \quad . \tag{8}$$

Use of Equations (1), (6), and (8) gives

$$\epsilon = p\theta \quad . \tag{9}$$

Evaluation of Equations (6), (8), and (9) for several values of n gives the results in Table 1. The experimental and theoretical indications for NO^+ and O_2^+ are that $\frac{1}{2} \leq p \leq 1$ and hence that $\frac{1}{2} \leq \epsilon/\theta \leq 1$.

As a practical matter, however, the dissociative-recombination heating rate may be insensitive to the particular power-law rate coefficient used. For example, consider rate coefficients $k_1 = k_{01}\,\theta^{-p_1}$ and $k_2 = k_{02}\,\theta^{-p_2}$; define θ_k and θ_{kp} to be the temperatures for which the respective equalities $k_1 = k_2$ and $k_1 p_1 = k_2 p_2$ are satisfied, and define R to be the ratio of the heating rates, $R \equiv \dot{H}_1/\dot{H}_2 = k_1 p_1 / k_2 p_2$. If $p_1 < p_2$, then $R < 1$ for $\theta < \theta_k$ but R increases for $\theta > \theta_k$ until $R = 1$ at $\theta = \theta_{kp}$ and $R > 1$ for $\theta > \theta_{kp}$. Thus, if the problem of interest is one for which the temperature has a small range about θ_{kp}, then the heating due to dissociative recombination will depend little on the choice made for k.

In Fig. 1 we illustrate the magnitude of dissociative-recombination heating relative to other heating and cooling mechanisms for ionospheric electrons. The usual heating- and cooling-rate curves in Fig. 1 are those computed by Timothy et al. (1972) for their rocket flight. To compute the

curve for dissociative-recombination heating, we used the densities and temperatures given by Timothy et al. (1972): values of [e], $[NO^+]$, and $[O_2^+]$ were taken from Table 11 (temperature-condition c); values of θ were taken from Fig. 37 (measured values for $h > 150$ km and calculated values for $h \leq 150$ km). We used

$$k(NO^+) = 4.0 \times 10^{-7} (T/300)^{-0.8} \quad (10)$$

$$k(O_2^+) = 2.1 \times 10^{-7} (T/300)^{-0.7} \quad (11)$$

for the dissociative-recombination rate coefficients (Bortner et al., 1973) and Equation (4) for each of the heating-rate contributions from NO^+ and O_2^+. We see that the heating rate due to dissociative recombination is a small fraction (from 2.6 to 5.3 per cent) of the main heating rate due to photoelectrons but that it does exceed some of the rates for minor cooling processes frequently included in energy-balance studies.

After completing this work, we noted a comment by Dalgarno (1973) that relates closely to the topic discussed here, though it was made in an astrophysical context with respect to radiative recombination: "The cold electrons recombine more readily and recombination is itself a mechanism for increasing T_e [the electron temperature]."

Acknowledgement — This work was partially supported by the Defense Advanced Research Projects Agency of the Department of Defense and was monitored by ONR under Contract No. N00014-72-C-0292.

REFERENCES

Bortner, M. H., Kummler, R. H. and Baurer, T. (1973). Summary of suggested rate constants in Defense Nuclear Agency Reaction Rate Handbook, DNA 1948H (Eds. M. H. Bortner and T. Baurer), Second edition (Revision No. 2, in press), Ch. 24. Defense Nuclear Agency, Washington, D. C.

Dalgarno, A. (1973). Atomic processes in astrophysics, in Brandeis University Summer Institute in Theoretical Physics, 1969: Vol. 2, Atomic Physics and Astrophysics, p. 285. Gordon and Breach Science Publishers, New York.

Stubbe, P. and Varnum, W. S. (1972). Electron energy transfer rates in the ionosphere, Planet. Space Sci. 20, 1121.

Timothy, A. F., Timothy, J. G., Willmore, A. P. and Wager, J. H. (1972). The ion chemistry and thermal balance of the E- and lower F-regions of the daytime ionosphere: An experimental study. J. atmos. terr. Phys. 34, 969.

TABLE 1. Parameters for Effective Energy-Return to Electron Gas for Power-Law Dissociative-Recombination Cross-Section

n^*	$p^\dagger = \epsilon/\theta$	$\langle E \rangle/\theta$
$-\frac{1}{2}$	-1	$\frac{5}{2}$
0	$-\frac{1}{2}$	2
$\frac{1}{2}$	0	$\frac{3}{2}$
1	$\frac{1}{2}$	1
$\frac{3}{2}$	1	$\frac{1}{2}$

*Exponent in Equation (5).

†Exponent in Equation (7).

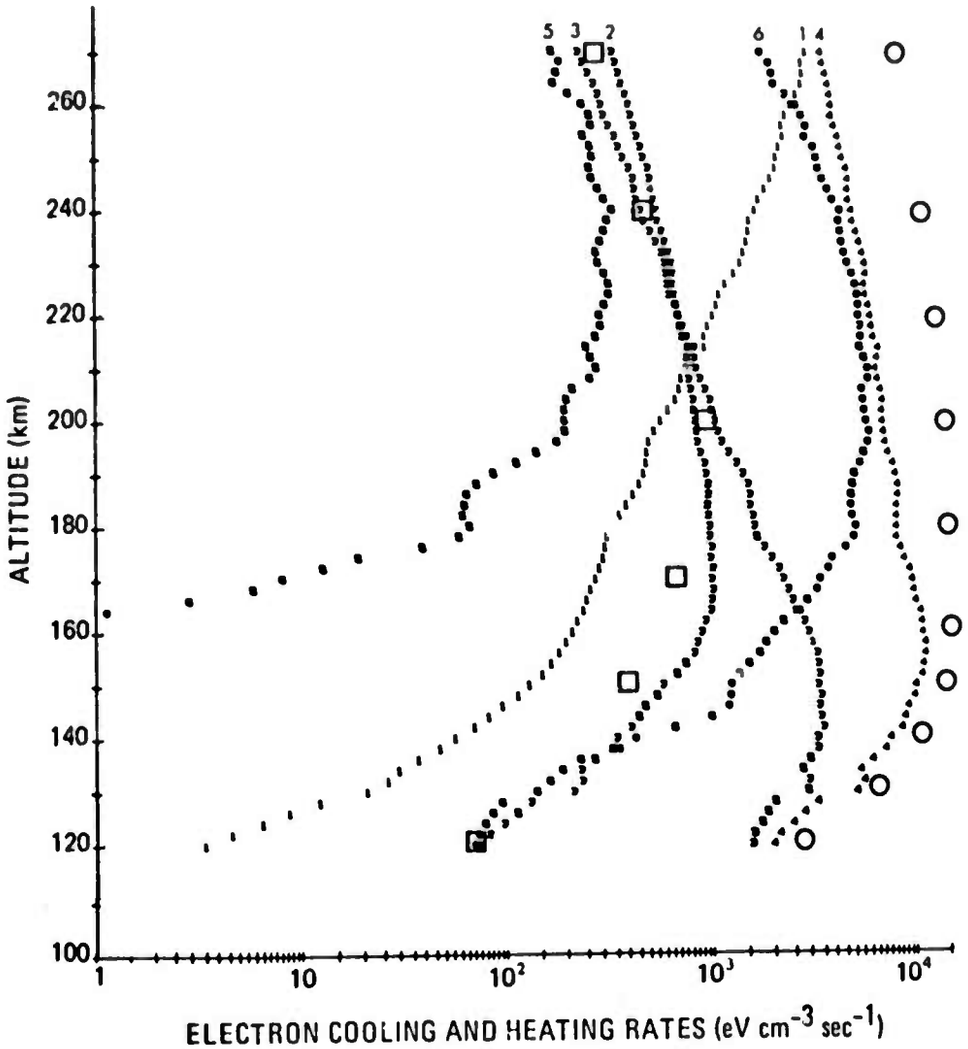

Fig. 1. Calculated cooling and heating rates for ambient electrons. Cooling rates (Timothy et al., 1972; Fig. 38): (1) elastic (positive ions); (2) elastic (neutrals); (3) rotational excitation; (4) fine-structure excitation; (5) electronic excitation; (6) vibrational excitation. Heating rates: O photoelectrons (Timothy et al., 1972, Fig. 27); □ dissociative recombination (see text)

SECTION 5

TEMPERATURE DEPENDENCE FOR DISSOCIATIVE RECOMBINATION OF NO^+ IN E- AND F-REGION MODELS

Temperature Dependence for Dissociative Recombination of NO^+ in E- and F-Region Models†

B. F. Myers
Science Applications, Inc.
La Jolla, California 92037, U. S. A.

Abstract — A discussion is given which indicates that the temperature dependence for the dissociative recombination of NO^+ customarily used in E- and F-region models is not correct.

Recent atmospheric models, such as Torr and Torr (1969), Keneshea et al. (1970), Stubbe (1970), Nisbet (1971) and Rüster (1971), which include a description of chemistry in the E- and F-regions, use a temperature* dependence of T^{-1} or $T^{-\frac{3}{2}}$ for the rate coefficient of dissociative recombination of NO^+. On the basis of present experimental and theoretical evidence (Bardsley, 1970; Bardsley and Biondi, 1970), these temperature dependencies are incorrect for temperatures to be encountered in the E- and F-regions.

The appropriate temperature dependence of the rate coefficient should be that for the dissociative recombination of NO^+ which is essentially in the ground vibrational state. Although the temperatures in the E- and F-regions correspond only to a small degree of vibrational excitation of NO^+ under the assumption of equilibration of energy modes, this is not a sufficient basis for the preceding recommendation. The formation of NO^+ is principally by way of the processes

*The temperature is specifically the electron temperature under conditions of nonequilibrium among the translational modes of electrons, ions and neutral particles.

†Published in Journal of Atmospheric and Terrestrial Physics, 1973, Vol. 35, pp. 1903-1904. Pergamon Press.

$$N_2^+ + O \rightarrow NO^+ + N \quad (1)$$

$$O_2^+ + NO \rightarrow O_2 + NO^+ \quad (2)$$

$$O^+ + N_2 \rightarrow NO^+ + N \quad . \quad (3)$$

Reactions (1) and (2) have large rate coefficients and are highly exothermic. Consequently, the product NO^+ may be formed with energy in the vibrational mode much in excess of that corresponding to E- and F-region temperatures. This possibility cannot be dismissed on the basis of present experimental results and for reaction (2) current knowledge about charge transfer processes involving molecular species supports the possibility (Rutherford et al., 1971; Tomcho and Haugh, 1972). For reaction (3), which has a smaller rate coefficient and is less exothermic than either reactions (1) or (2), recent experiments (Neynaber and Magnuson, 1973) indicate that for most of the NO^+ produced, 75 per cent or more of the available energy (reaction exothermicity, vibrational energy of N_2 and relative kinetic energy of reactants) may be transferred to internal modes of NO^+. If NO^+ is formed with substantial energy in vibrational modes, and if there were no way to remove this energy before dissociative recombination, the rate coefficient to be used could be significantly different (O'Malley, 1969; Bardsley, 1970) from the case with energy in the vibrational modes corresponding to E- and F-region temperatures. Thus, in the absence of definitive experimental results for the distribution of energy among the products of reactants (1), (2) and (3), and of redistribution of energy involving vibrational modes of NO^+ prior to dissociative recombination, no recommendation could apparently be made concerning the temperature dependence. However, in spite of the possibility for forming NO^+ in vibrationally excited levels, when undergoing dissociative recombination the NO^+ will be in the ground vibrational state, on the average, as a result of radiative decay. Radiative decay of vibrationally excited NO^+ molecules occurs in the infrared spectral region with frequencies of

the order of 10^2 sec^{-1} (Herzberg, 1950; Miescher, 1956; Penner, 1959; Stair and Gauvin, 1967); consequently radiative decay will predominate, even ignoring energetic and transition-probability considerations, at altitudes above about 120 km, where the collision frequencies ($\leq 10^2$ sec^{-1}) are smaller than radiative decay frequencies.

Just what temperature dependence should be used in E- and F-region models remains to be firmly established. Perhaps a $T^{-\frac{1}{2}}$ dependence indicated by theory (Bardsley, 1970) could be used in the interim.

Acknowledgements — The author is grateful to Drs. D. A. Hamlin, R. H. Neynaber and J. I. Valerio for helpful discussions. This research was partially supported by the Advanced Research Projects Agency of the Department of Defense and was monitored by ONR under Contract No. N00014-72-C-0292.

REFERENCES

Bardsley J. N.	1970	Phys. Rev. A2, 1359.
Bardsley J. N. and Biondi M. A.	1970	Adv. atom. mol. Phys. 6, 1.
Herzberg G.	1950	Molecular Spectra and Molecular Structure, Vol. I. Spectra of Diatomic Molecules (2nd edn.), p. 92. Van Nostrand, Princeton, N. J.
Keneshea T. J., Narcisi R. S. and Swider W., Jr.	1970	J. geophys. Res. 75, 845.
Miescher E.	1956	Helv. Phys. Acta 29, 135.
Neynaber R. H. and Magnuson G. D.	1973	J. chem. Phys. 58, 4586.
Nisbet J. S.	1971	Radio Sci. 6, 437.
O'Malley T. F.	1969	Phys. Rev. 185, 101.
Penner S. S.	1959	Quantitative Molecular Spectroscopy and Gas Emissivities, p. 21. Addison-Wesley, Reading, Mass.
Rüster R.	1971	J. atmos. terr. Phys. 33, 137.
Rutherford J. A., Mathis R. F., Turner B. R. and Vroom D. A.	1971	J. chem. Phys. 55, 3785.
Stair A. T., Jr. and Gauvin H. P.	1967	Aurora and Airglow (Edited by B. M. McCormac), p. 365. Reinhold, New York.
Stubbe P.	1970	J. atmos. terr. Phys. 32, 865.
Tomcho L. and Haugh M. J.	1972	J. chem. Phys. 56, 6089.
Torr M. R. and Torr D. G.	1969	J. atmos. terr. Phys. 31, 611.